ADVANCED MATERIALS
www.advmat.de

Superhydrophobic Solar-to-Thermal Materials Toward Cutting-Edge Applications

Shan Li, Peng Xiao, and Tao Chen**

Dedicated to the 20th anniversary of the Ningbo Institute of Materials Technology and Engineering

Solar-to-thermal conversion is a direct and effective way to absorb sunlight for heat via the rational design and control of photothermal materials. However, when exposed to water-existed conditions, the conventional solar-to-thermal performance may experience severe degradation owing to the high specific heat capacity of water. To tackle with the challenge, the water-repellent function is introduced to construct superhydrophobic solar-to-thermal materials (SSTMs) for achieving stable heating, and even, for creating new application possibilities under water droplets, sweat, seawater, and ice environments. An in-depth review of cutting-edge research of SSTMs is given, focusing on synergetic functions, typical construction methods, and cutting-edge potentials based on water medium. Moreover, the current challenges and future prospects based on SSTMs are also carefully discussed.

1. Introduction

Solar energy is a green, renewable, and inexhaustible resource that can be easily captured to realize diverse photovoltaic and photothermal conversion.[1] As a direct and efficient technology, solar-to-thermal conversion can convert incident sunlight into considerable thermal energy by the introduction of well-designed light-absorbing materials.[2] Among them, carbon nanomaterials,[3] conjugated polymers,[4] and plasmon resonance nanoparticles[5] are widely applied owing to their high photothermal conversion efficiency,[6] showing a variety of potentials in functional surfaces, thermal management devices, and so on.

As conventional photothermal materials with hydrophilic or hydrophobic wettability show considerable thermal losses to water due to the high specific heat capacity, their efficiencies and application potentials are severely limited. A typical example of wearable thermal management devices wetted by water molecules can experience a sharp decrease of the surface temperature and cannot generate enough thermal energy for radiative heating. Another example shows that when applied on water surface for specific applications such as solar evaporators or light-driven actuators, almost all the thermal energy can be absorbed by the bulk water. Although water can seriously weaken the solar-to-thermal performance, the photothermal materials applied under water conditions are inevitable. In addition, a series of new and meaningful applications can be created based on the water environment. Therefore, the development of water-repellent photothermal materials is highly desired for exploiting the water-based solar-to-thermal applications.

Specifically, the introduction of superhydrophobic structure into the solar-to-thermal materials system is expected to be conducive to the implementation of continuous and stable thermal supply.[7] Superhydrophobic solar-to-thermal materials (SSTMs) featured with hierarchical micro–nano structures can demonstrate the capabilities of enhanced light capture and water repellency to tackle with the unfavorable water disturbance. As illustrated in **Figure 1**, multilevel micro–nano structural surface can remarkably trap sunlight into the hierarchical structure, enhance sunlight absorption with multiple light reflections, and further achieve remarkably enhanced solar-to-thermal efficiency. On the other hand, the micro–nano structures can effectively form air layers to prevent the water infiltration, allowing falling water droplets on SSTMs to be quickly bounced away. Benefitting from the synergetic effect of the two functions, SSTMs show the capabilities of thoroughly repelling water and further maintaining stable solar heating under diverse water conditions. The well-designed SSTMs are expected to present the typical advantages on the water-related environments (e.g., water droplets, water surfaces, and even ice surfaces) and applications, such as anticing and deicing,[8] seawater desalination,[9] soft actuators,[10] efficient energy utilization,[11] and biomedicine.[12]

Although there have been many reviews of the individual superhydrophobic surfaces[13] or solar-to-thermal materials,[14] the systematic introduction of SSTMs with synergetic functions, typical design strategies, and cutting-edge applications has not been summarized. As a member of photothermal materials, the SSTMs demonstrate typical feature of water-repellent solar

S. Li, P. Xiao, T. Chen
Key Laboratory of Advanced Marine Materials
Ningbo Institute of Materials Technology and Engineering
Chinese Academy of Sciences
Ningbo 315201, China
E-mail: xiaopeng@nimte.ac.cn; tao.chen@nimte.ac.cn
S. Li, P. Xiao, T. Chen
School of Chemical Sciences
University of Chinese Academy of Sciences
19A Yuquan Road, Beijing 100049, China

The ORCID identification number(s) for the author(s) of this article can be found under https://doi.org/10.1002/adma.202311453

DOI: 10.1002/adma.202311453

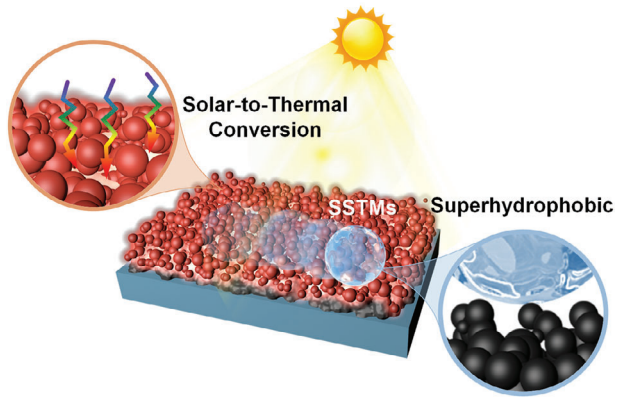

Figure 1. Schematic illustration of SSTMs with multilevel micro–nano structural surface for enhanced solar-to-thermal conversion and water repellency properties.

heating function, which can remarkably broaden the water-related application field. Our research group has been dedicated to exploiting solar-to-thermal materials, and especially, to focusing on the construction of a series of SSTMs for seawater desalination, thermal management, and light-driven soft actuators.[11,15] This review provides a tutorial overview that summarizes the recent progress in SSTMs, focusing on the construction methods for superhydrophobic solar-to-thermal surface and their cutting-edge applications under diverse water condition. A systemic framework of SSTMs with construction methods and potential applications is schematically depicted in **Figure 2**, in which SSTMs can effectively absorb sunlight to generate considerable thermal energy and further prevent the wetting of water droplets. In addition, the construction strategies of SSTMs are introduced in detail, including laser-etching, spraying, salt template, chemical deposition, dip-coating, and layer-by-layer assembly. Owing to the synergetic functions of SSTMs, a series of water-related applications is comprehensively described to achieve stable and high-efficient utilization of solar energy, aiming to work in cutting-edge fields of anti-icing and deicing, seawater desalination, crude oil collection, light-driven actuators, wearable devices, indoor thermal management, and sterilization. This review is ended by summarizing the ongoing challenges of SSTMs along with a perspective in future research. With this review, we hope that the typical characteristic of SSTMs inspires new ideas and efforts and attracts more like-minded researchers.

2. Basic Compositions of SSTMs

2.1. Solar-to-Thermal Conversion Materials

The sun emits photons with different vibratory frequencies to supply energy for the Earth, including ultraviolet (UV), visible light (Vis), and infrared (IR).[16] Solar-to-thermal conversion materials can absorb solar photons and convert them to thermal energy for reutilizing, and their photothermal performance is primarily determined by the sunlight-collecting ability and the photothermal conversion efficiency.[17] Optical properties of the materials can be regulated via the absorption coefficient, reflectivity, and transmittance. Therefore, to improve solar-to-thermal conversion efficiency, materials with photothermal property should meet the characteristics of high broadband (300–2500 nm) solar absorption and low transmission/reflectivity (**Figure 3**a), and its solar-collecting ability can be further enhanced by constructing multistage micro–nano structures.[14b] For instance, Xiao et al. developed a hierarchical polypyrrole nanospheres structure that possessed higher than 96% sunlight absorption and less than 4% reflection due to the enhanced sunlight capture via multiple interstitials inside (Figure 3b).[18]

The most commonly used photothermal conversion mechanisms include plasma local heating (metallic materials), non-radiative relaxation (semiconductors), and molecular thermal vibration (carbon and organic polymer materials) (Figure 3c). Specifically, when the vibration frequency of the incident sunlight matches with the resonance frequency of the free electrons in the metal conduction band, the free electrons will oscillate coherently or undergo the surface plasmon resonance (SPR) to produce hot electrons. The vibrating hot electrons radiate electromagnetic waves, thereby resulting in a rapid increase in the temperature of the local surface.[5] Semiconductor materials release heat in the form of electron–phonon coupling through non-radiative relaxation of electron–hole pairs in the band gap.[19] As for conjugated carbon and organic polymer materials, the excited electrons by sunlight tend to release the absorbed energy; and thus, experience a non-radiative transition from the excited state to the ground state. This transition is accompanied by the release of heat energy.[20] The above three photothermal mechanisms are based on the optics of specific materials.

2.2. Superhydrophobic Surface

When a droplet falls on a solid surface, the angle between the liquid–gas interface and the liquid–solid interface is defined as the contact angle (CA). The surfaces with a contact angle of more than 150° and a rolling angle of less than 10° are known as a superhydrophobic surfaces, which cannot be wetted by a liquid.[13a,c] The mechanism of superhydrophobic material is systematically summarized in **Figure 4**. First, Young researched the surface wettability and further summarized the relationship among the contact angle of solid, liquid, and gas and the interfacial tension in 1805,[21] which can be expressed as

$$\cos\theta = \frac{\gamma_{SV} - \gamma_{SL}}{\gamma_{LV}} \quad (1)$$

where θ is the contact angle and γ_{SL} is the interfacial tension between solid and liquid. γ_{SV} is the interfacial tension between solid and gas, and γ_{LV} is the liquid–gas interfacial tension. However, the Young's equation is only suitable for surfaces with uniform and smooth chemical composition, which are difficult to apply for rough surfaces in practical applications. Therefore, Wenzel modified Young's equation by introducing a term: roughness factor r (ratio of actual solid–liquid contact area to apparent solid–liquid contact area),[22] which is shown as follows

$$\cos\theta^* = r\cos\theta \quad (2)$$

where θ* is the apparent contact angle of the rough surface. The Wenzel equation is consistent with the Young's equation when

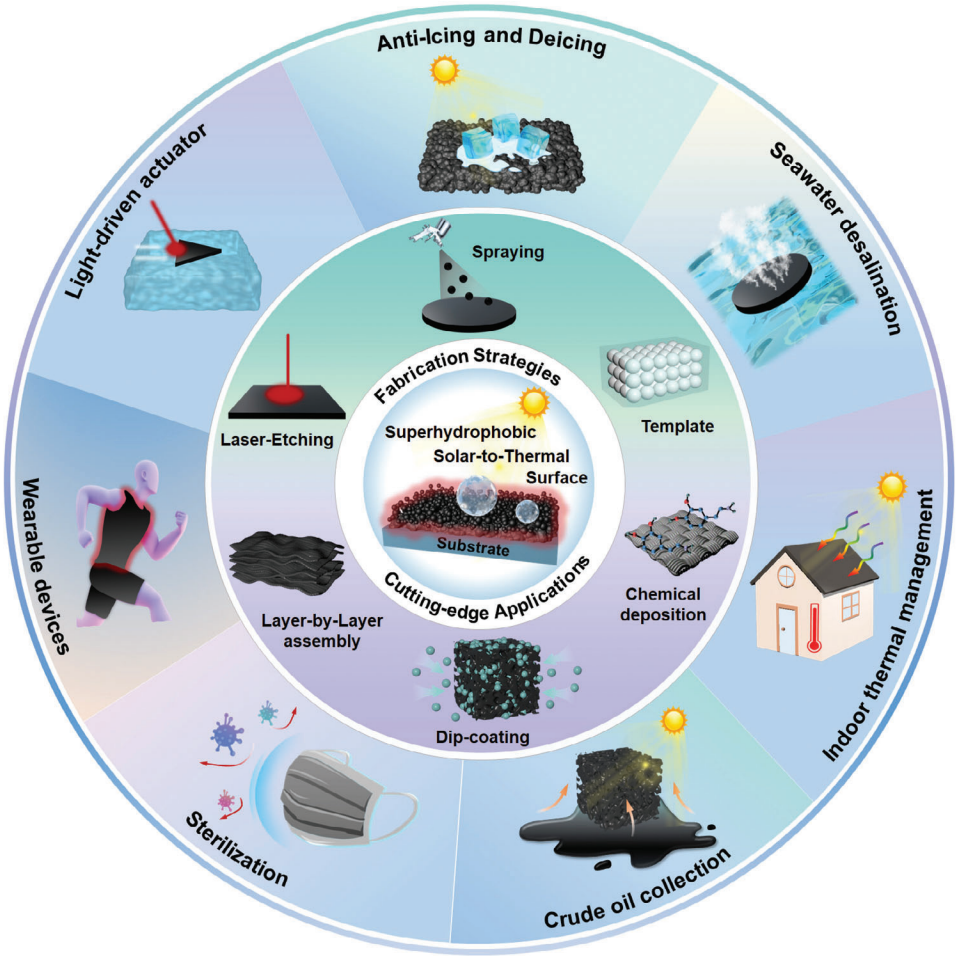

Figure 2. Overview of fabrication strategies and cutting-edge applications of SSTMs, including top–down methods (laser etching, spraying, and template method) and bottom–up methods (chemical deposition, dip-coating, and layer-by-layer assembly), that can be utilized for anti-icing and deicing, seawater desalination, crude oil collection, light-driven actuators, wearable devices, indoor thermal management, and sterilization.

the solid surface is ideally smooth ($r = 1$). From the Equation (2), it can be easily obtained that, with the surface roughness increasing, the hydrophilic surface tends to be super-hydrophilic and the hydrophobic surface tends to be super-hydrophobic. However, many other wetting phenomena in nature cannot be explained by the Wenzel equation, such as the lotus effect.

Owing to the limitations of Wenzel equation, Cassie and Baxter[23] further generalized the Wenzel equation. Due to the sufficient micro and nano structures on the surface, the droplets only contact the top of the trench and the air layer trapped at the bottom, which forms the solid–liquid-gas three-phase composite interface. Therefore, Cassie and Baxter introduced the solid–liquid contact area fraction (f_1) and gas–liquid contact area fraction ($f_2, f_1 + f_2 = 1$). The Cassie–Baxter equation is as follows

$$\cos\theta^* = f_1 \cos\theta_1 + f_2 \cos\theta_2 \tag{3}$$

where θ_1 and θ_2 are the contact angles of solid–liquid and liquid–gas. Currently, Cassie–Baxter's theory is widely applied theoretical framework for understanding the superhydrophobic structure and mechanism. Owing to the tiny contact area and air-film between the droplet and the solid, the droplet can easily bounce and roll away from the superhydrophobic surface, showing potential applications in self-cleaning,[24] anti-icing,[13a,25] biomedicine,[26] and so on. Based on the above equations, in our review, we work on constructing photothermal surfaces with superhydrophobic properties. The preparation methods for achieving SSTMs are discussed in the following section.

3. Design and Construction of SSTMs

The key factors for fabricating SSTMs are the construction of multilevel micro–nano structures as well as low surface energy.[27] Currently, the methods for fabricating photothermal superhydrophobic surfaces are divided into two categories, including the construction of appropriate micro–nano rough structures on the surface of low surface energy materials (top–down methods) and the modification of low surface energy materials on the rough surface (bottom–up methods). Top–down methods include laser etching, spraying and template methods, and bottom–up approaches have chemical deposition, dip-coating, and layer-by-layer assembly. Further, the constructed rough

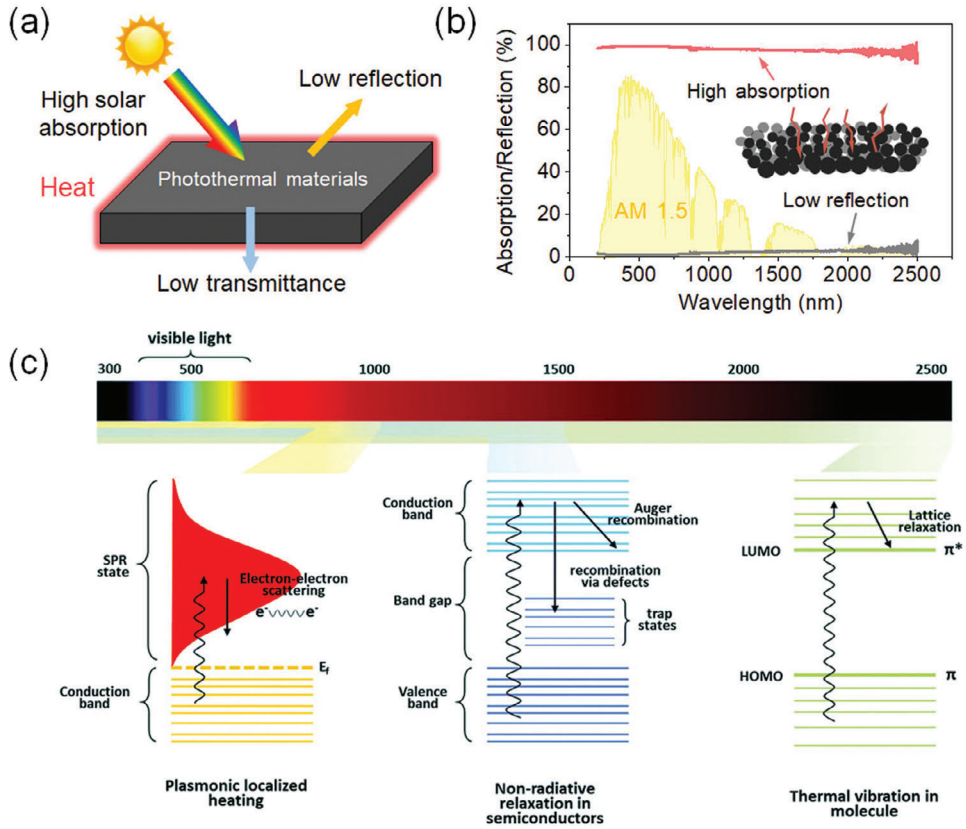

Figure 3. Solar-to-thermal conversion materials and their working mechanisms. a) Basic characteristics of photothermal materials. b) Optical properties of photothermal materials with multistage micro–nano structure. Reproduced with permission.[18] Copyright 2022, American Chemical Society. c) Three common mechanisms of solar-to-thermal conversion materials. Reproduced with permission.[14d] Copyright 2019, Royal Society of Chemistry.

structure can enhance the ability of photothermal materials to capture sunlight in a certain extent, which proves the functional enhancement and coordination of the superhydrophobic surface and solar-to-thermal conversion materials. The preparation strategies of SSTMs are summarized and analyzed, along with their pros and cons, according to the recent progress in this area.

3.1. Top–Down Methods

3.1.1. Laser-Etching

The most common method for preparing SSTMs is laser etching, which can construct micro–nano structures by direct laser radiation on the substrate surface. Due to the high energy and high density of the laser, the superhydrophobic solar-to-thermal surfaces can be effectively obtained via laser ablation and melting.[28] By adjusting the energy density, scanning rate, scanning distance, and spot size of the laser beam, multilevel micro–nano structural surface can be easily realized. Rigid metals (e.g., titanium and copper) and flexible polymers (e.g., PDMS, PTFE, and PI) are typical substrate materials, which can be carbonized by laser ablation to obtain the photothermal micro–nano structures.[29] In the following, the preparation schematic for constructing SSTMs on flexible and rigid substrates by laser etching will be illustrated and complemented.[30]

As shown in **Figure 5**a, a one-step laser processing was reported to etch the polytetrafluoroethylene (PTFE) surface

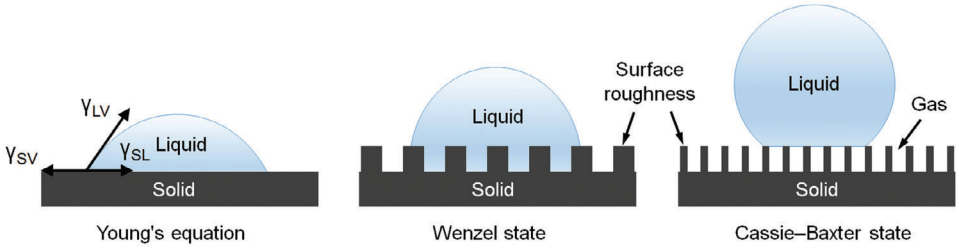

Figure 4. Solid surface wetting principles, including Young's equation, Wenzel state, and Cassie–Baxter state. The superhydrophobic surface belongs to the Cassie–Baxter state, which can be achieved by the construction of multistage micro and nano structures and low surface energy materials.

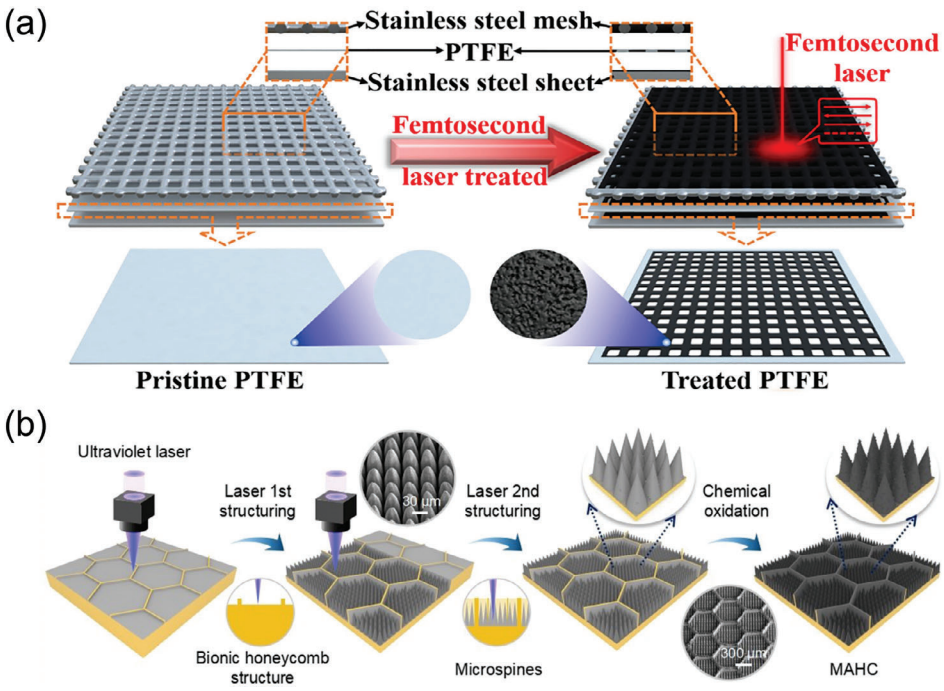

Figure 5. Preparation diagrams of SSTMs by laser etching method, including based on the flexible and rigid substrates. a) Design and construction principles of flexible superhydrophobic solar-to-thermal PTFE membrane via laser-etching. Reproduced with permission.[31] Copyright 2022, Elsevier. b) Schematic illustration of MAHC with robust honeycomb structures via multistage laser etching and chemical oxidation. Adapted with permission.[32] Copyright 2023, John Wiley and Sons.

covered with stainless steel mesh, thereby realizing a porous superhydrophobic PTFE membrane with a mesh pattern.[31] The micro–nano structured metal particles by laser treatment were alternatively deposited on the PTFE surface, which endowed PTFE membrane with enhanced light absorption. When the nanoparticles were embedded into the micro-scale porous structure, the PTFE membrane could demonstrate both water repellency and air permeability. The well-designed mask overcame the problem from low laser accuracy and infertile patterns, which was suitable for flexible substrates with low melting point and thin thickness. However, exposed nanoparticles of flexible superhydrophobic surfaces exposed usually exhibit weak bonding forces and robustness; thus, the introduction of rigid structures is usually an effective solution to this problem.

The rigid substrates exhibit superior resistance to friction, bending and durability, providing a convenient mode and low laser power to create superhydrophobic solar-to-thermal structures. As displayed in Figure 5b, inspired by the honeycomb hexagons and superhydrophobic micro-spine on cactus thorn, a robust photothermal icephobic surface with mechanical durability (MAHC) was developed via a laser-layered microfabrication strategy.[32] Under the protection of hard bionic copper honeycomb structure, the micro-spine array maintained its original structure and the superior water repellency property even after 200 linear abrasion cycles, providing a new method for designing durable SSTMs.

Laser etching presents an appealing choice for superhydrophobic solar-to-thermal surfaces due to its convenient, efficient, environmentally-friendly properties, and so on. Further, the construction strategy of SSTMs can be applied in diverse substrates. It is worth noting that the mechanical stability of the superhydrophobic micro–nano structures should be further improved.

3.1.2. Spraying

The superhydrophobic surface can be achieved by spraying a solution with micro–nano particles onto the targeted substrates. To obtain high photothermal conversion efficiency, the raw materials with solar-to-thermal conversion, such as CNTs,[33] graphene oxide,[8a] carbon fiber powder (CFP),[34] and Mxene,[35] are adopted to construct SSTMs on arbitrary substrates via spraying technology. One strategy is constructing solar-to-thermal coating with solar-to-thermal raw materials, and then, spraying nanoparticles to achieve multilevel micro–nano structures. As shown in **Figure 6a**, melanin nanoparticles with a wide range of light absorption capacity dispersed in PDMS were sprayed onto the substrate surface to achieve the stable solar-to-thermal coating.[36] Moreover, the hydrophobic silica nanoparticles were further sprayed to obtain the superhydrophobic solar-to-thermal surface structures. Among them, melanin particles endowed the coating with micro-scale structures and solar-to-thermal ability, and silica nanoparticles contributed to the roughness and low surface energy for SSTMs. In another strategy, a superhydrophobic solar-to-thermal coating could be prepared by spraying a mixture of beeswax, multi-walled carbon nanotubes (MCNTs), and polydimethylsiloxane (PDMS) on various substrates (e.g., glass, plastic, and wood) (Figure 6b).[37] With the solvent volatilization, the formed coating with micro–nano structures possessed solar-to-thermal conversion efficiency

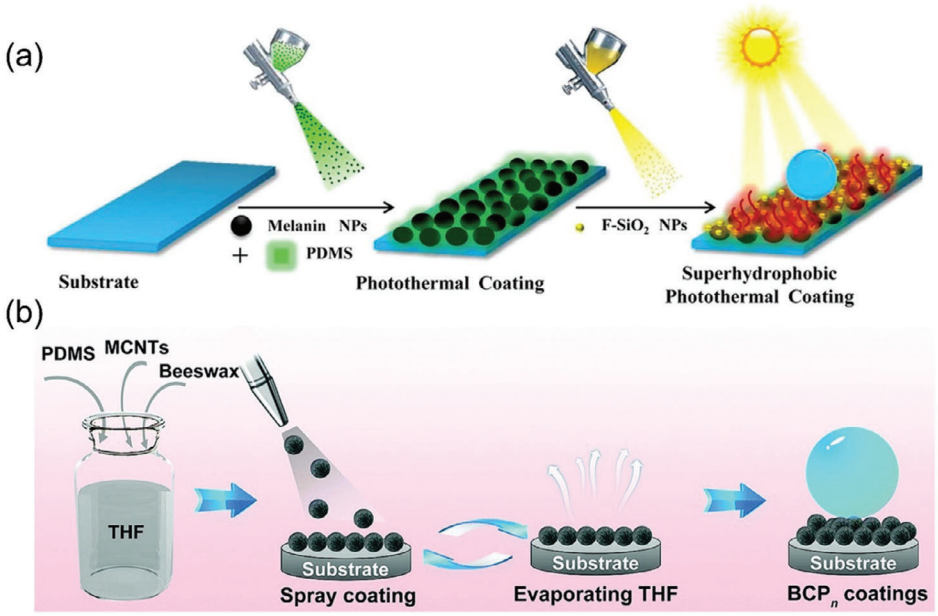

Figure 6. Strategy for preparing SSTMs based on spraying. a) Schematic illustration of superhydrophobic solar-to-thermal coatings by two-step spraying method. Reproduced with permission.[36] Copyright 2021, Elsevier. b) The fabrication process of self-healing superhydrophobic solar-to-thermal coating by one-step spraying. Reproduced with permission.[37] Copyright 2012, Royal Society of Chemistry.

of 88.2% and self-cleaning ability. Importantly, the prepared coating showed self-healing superhydrophobic ability, which could spontaneously repair superhydrophobic damage through the migration of beeswax when the surface was damaged.

Currently, spraying is a conventional technology for fabricating SSTMs on flat surfaces due to its advantages of convenient operation, low-cost, repairability, large-scale production, and so on. Achieving the uniformity of spraying coatings on complex curved surfaces poses a significant challenge that requires further exploration and research. In addition, the parameters (e.g., pressure, distance, and angle) of spraying play a crucial role in determining the adhesion of the coating to the substrate, which may result in unavoidable waste of raw materials.

Another top–down approach of salt templating is adopted to construct porous microstructures of SSTMs by filling the pores with filler, and then, removing the salt template. For example, the carbon-based SSTMs with surface microporous array structure and thermal insulation can be obtained by the nano carbon powder (CNP) with remarkable sunlight absorption rate as the solar-to-thermal material and PDMS as the binder to fill the gap in the template.[38] Note that owing to the high solubility of NaCl, the salt template method is simple and convenient to remove the template. Nevertheless, there are limited studies to meet the requirements of SSTMs.

3.2. Bottom–Up Methods

3.2.1. Chemical Deposition

Three main categories of chemical deposition include chemical vapor deposition (CVD), electrochemical deposition, and liquid phase deposition, which can be further combined with hydrophobic agents to reduce the surface energy and improve the stability of coatings. As displayed in **Figure** 7a, He's group fabricated a superhydrophobic solar thermal coating with high photothermal efficiency via CVD and surface grafting strategies.[39] The tetraethoxysilane (TEOS) was introduced to the candle soot with hierarchical micro–nano structures to enhance the stability of the CS layer. The hierarchical structures of superhydrophobic candle soot could remarkably improve light absorption efficiency, and the grafted PDMS onto the surface endowed the coating with low surface energy and superhydrophobicity. A recent study via electrochemical deposition reported a superhydrophobic solar-to-thermal fabric with growing carbon nanowire arrays (CA) on carbon cloth (CC) to achieve micro–nano structures and low surface energy through silanization treatment (Figure 7b).[40] The hierarchical structures, composed of black carbon-based materials with extensive light absorption properties, could effectively enhance light harvesting and readily demonstrate achievement of carbon-based SSTMs with favorable anti-icing and solar-to-thermal deicing properties. Moreover, a superhydrophobic solar-to-thermal polyurethane sponge was prepared by liquid phase depositing Fe_3O_4 nanoparticles and polydopamine (PDA) (Figure 7c).[41] The combination of nanoparticles and polydopamine not only provided the nanostructures but also enhanced the photothermal conversion capability of the sponge.

Recently, inspired by the tightly packed melanosome structure of black fish, our research group developed a super-hydrophobic solar-to-thermal fabric with the hierarchical structure of polypyrrole (Ppy) nanospheres.[15f] The nanoscale gaps within the synthetic melanosome layer allowed highly scattered incident light and enhanced absorption of up to 96%. Further, the biomimetic hierarchical textile exhibited good superhydrophobicity and

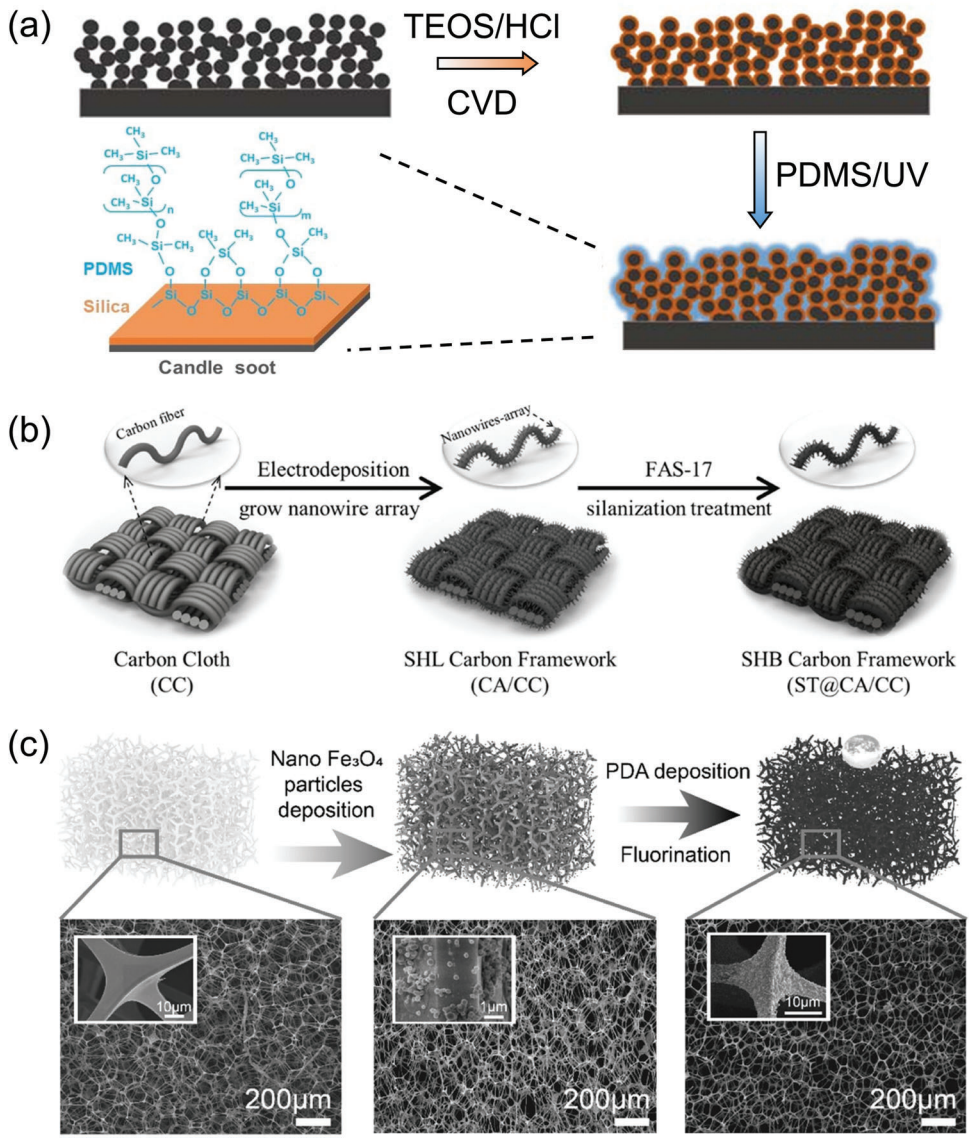

Figure 7. Schematic diagram for the preparation of SSTMs via chemical deposition. a) Fabrication and structure schematic diagrams of superhydrophobic solar-to-thermal coating by chemical vapor deposition. Reproduced with permission.[39] Copyright 2020, National Academy of Sciences. b) The fabrication process of the superhydrophobic solar-to-thermal fabric using electrochemical deposition method. Reproduced with permission.[40] Copyright 2021, American Chemical Society. c) Schematic illustrations showing preparation and microstructures of superhydrophobic solar-to-thermal polyurethane sponge via liquid phase deposition. Reproduced with permission.[41] Copyright 2023, American Chemical Society.

enhanced photothermal and electrothermal properties, demonstrating significant potential in wearable thermal management in water conditions. However, the deposited nanostructures through the one-step solution reaction showed the brittleness and tendency to detach easily. Therefore, the improvement of the mechanical stability of SSTMs with robust performance is of significance.

Taken together, chemical deposition has been widely utilized to realize multilevel nano–micro structures due to its easy operation, good repeatability, and widespread applications. Among them, SSTMs via vapor deposition method, show the characteristics of uniform structure, corrosion resistance, and high purity, which can be employed to prepare alloy, ceramic, and polymer films. SSTMs via electrochemical deposition show significant potentials in magnetic and wear-resistant materials as well as in energy saving materials owing to the advantages of low-cost, safety, sustainability, material efficiency, and scalability. Liquid phase deposition is widely adopted to construct SSTMs with high-efficiency, low-cost, and compatibility, which shows broad applications in seawater desalination, anti-ice coatings, and more.

3.2.2. Dip-Coating

For sponges and fabrics with high BET or abundant end groups, dip-coating proves to be a practical approach. By immersing the

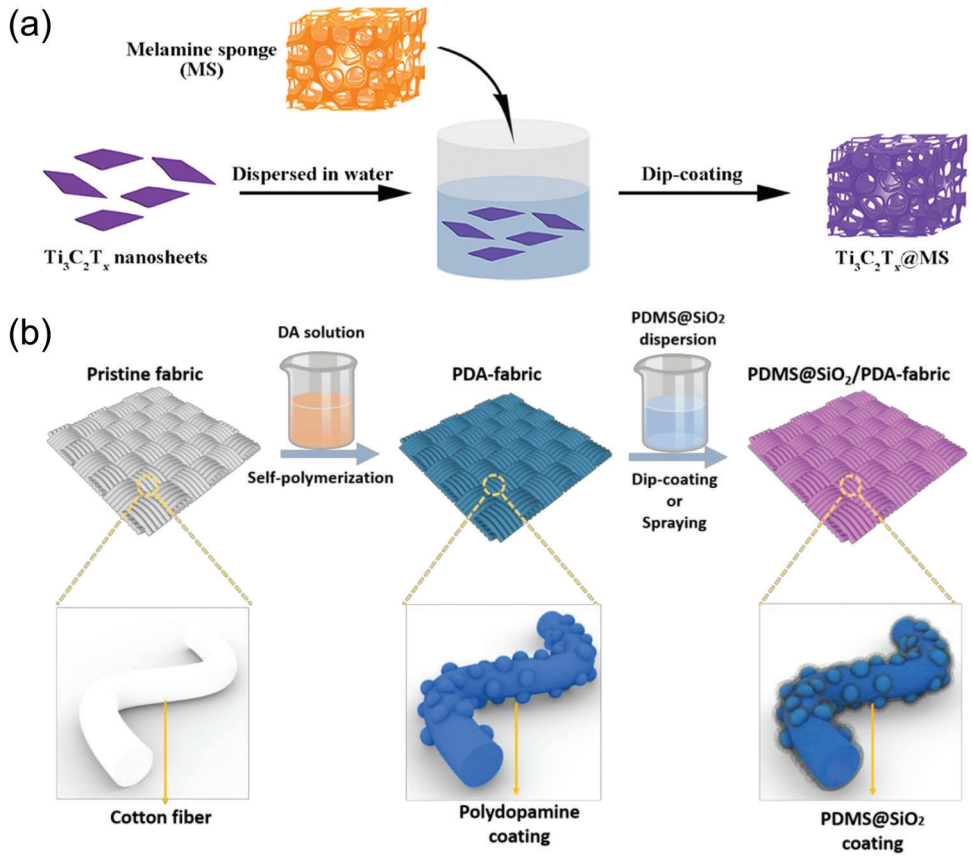

Figure 8. Schematic illustration for fabricating SSTMs by dip-coating. a) Preparation process of superhydrophobic solar-to-thermal sponge using dip-coating method. Reproduced with permission.[42] Copyright 2021, American Chemical Society. b) Schematic illustration of the fabrication of superhydrophobic solar-to-thermal textile using liquid-phase deposition and dip-coating. Reproduced with permission.[43] Copyright 2023, American Chemical Society.

raw materials into functional micro and nano particles dispersion, SSTMs can be obtained to allow functional particles to further permeate into the interior and surface through capillary forces or weak interactions (e.g., hydrogen bonding, ionic bonding, and hydrophobic forces). A typical example was reported to fabricate a superhydrophobic solar thermal sponge via dip-coating. As shown in **Figure** 8a, it can be clearly observed that the highly hydrophobic MXene-based sponge was obtained by dipping a melamine sponge (MS) into a dispersion solution of $Ti_3C_2T_x$ nanoparticles.[42] Owing to the abundant functional groups (—OH, —O, and —F) of MXene nanosheets, hydrogen bond interactions between the amino groups on the sponge skeleton and the polar groups on the surface of the $Ti_3C_2T_x$ nanosheets resulted in a rapid transition from hydrophilic to superhydrophobic of MS. Benefitting from high solar-to-thermal conversion efficiency of $Ti_3C_2T_x$, the modified sponge was endowed with superhydrophobicity and high solar-to-thermal efficiency. Moreover, hydrophilic fabrics may experience wettability transition and be loaded with solar-to-thermal functional components via dip-coating. For example, the superhydrophobic solar-to-thermal fabric could be realized via liquid phase depositing the PDA with high photothermal conversion efficiency and dipping in a PDMS@SiO_2 dispersion with a low surface energy (Figure 8b).[43] The adsorbed SiO_2 nano particles provided the hierarchical micro–nano structures to the fabric and endowed the fabric with superhydrophobic property. Due to the capacity for maximal raw material utilization, maneuverable equipment and sustainable production, dip-coating proves to be extensively employed for crude oil collection, seawater desalination, and individual thermal regulation.

3.2.3. Layer-by-Layer Assembly

Layer-by-layer assembly shows the capability of controlling the structure and properties of the assembly system at the molecular level, and it is not restricted by substrate and environment. By means of pressure and weak interactions (e.g., electrostatic force and hydrogen bonding), a disordered system can be converted into an ordered lamellar structure onto the substrate surface, resulting in a stable hierarchical system with superhydrophobic solar-to-thermal properties.

One example reported the method through electrostatic interactions between carboxyl groups and amino groups to deposit carboxylated and aminated multi-walled carbon nanotubes (MWCNT-COOH/MWCNT-NH_2) on the filter paper.[44] Then, the prepared MWCNT membrane was transferred to the EVA substrate to obtain multilevel micro–nano structures

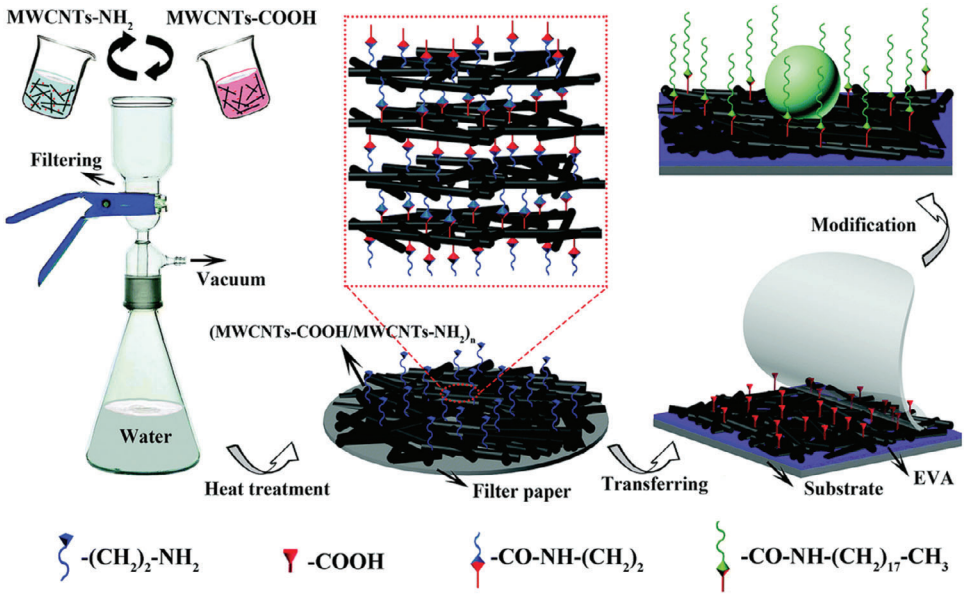

Figure 9. Fabrication illustration of SSTMs via layer-by-layer assembly. Schematic illustration for fabricating vacuum-assisted layer-by-layer superhydrophobic MWCNT films based on electrostatic interactions. Reproduced with permission.[44] Copyright 2012, Royal Society of Chemistry.

and exhibit the super-hydrophobicity with water contact angel of 165° (**Figure 9**). Thanks to the intrinsic solar-to-thermal conversion properties of MWCNT, the membrane could be used as a flexible actuator to move on water surface with Marangoni effect. Another example proposed layer-by-layer self-assembly with vacuum assisted filtration through hydrogen bonding between superhydrophobic MXene nanosheets by PFOTS grafting (MXene-F) and oxidized cellulose nanofibers (TOCNF), achieving photothermal superhydrophobic films with sandwich structure.[10a] Layer-by-layer assembly was considered to be a good alternative for preparing multifunctional films with characteristics of simple operation, low-cost, spontaneous processes, and controllable thickness. Therefore, layer-by-layer assembly showed great potential applications in seawater desalination, oil–water separation, and actuators.

Overall, the substrate category plays a crucial role in determining the appropriate approaches for SSTMs and defining their potential applications. The performance of materials obtained from the above preparation methods is compared and summarized in **Table 1**, which helps to establish an intuitive understanding about the differences between these strategies and provide a guidance for the design of superhydrophobic solar-to-thermal materials. Considering the fragility of the superhydrophobic micro–nano structures, the greatest obstacle posed by the aforementioned strategies is durability and mechanical stability. The introduction of polymer bonding layer to enhance the bonding force between superhydrophobic micro/nano structures and substrate is a mainstream solution, but it still depends on the stability of the top nanostructure. Deng et al. designed a protective microstructural "armor" featured with excellent mechanical properties and an interconnected frame, which successfully prevented the internal nanostructures from abrasion.[13e] This microstructural "armor" applies to various substrates and shows the effective water-repellency after abrasion by a sharp steel blade, providing a promising solution for constructing robust SSTMs.

4. Cutting-Edge Applications of SSTMs

SSTMs featured with solar-to-thermal property and water repellency can endow the material systems with a variety of functions and applications, such as anti-icing and deicing, seawater desalination, crude oil collection, light-driven actuators, and intelligent thermal management. Further, SSTMs are expected to provide a solution to global pathology problems such as antiseptic masks. In these applications, the role of the photothermal materials is to convert sunlight into considerable thermal energy and further heat ice, water, air, oil, and objects via a non-contact thermal radiation.[45] The superhydrophobic structures with hierarchical micro–nano structures and low surface energy exhibit many characteristics, such as water repellency, self-cleaning, enhanced sunlight absorption, reduced resistance, lipophilicity and reduced adhesion,[13a] which can further cooperate with photothermal conversion to achieve the performance improvement and application expansion of SSTMs.

4.1. Anti-Icing and Deicing

Icing is a common and inevitable phenomenon in nature. Undesirable ice accumulation will prevent from the normal performance of power lines, wind turbine blades, aircraft wings and roads, resulting in significant inconveniences to human life and even causing serious disasters or economic losses.[46] Consequently, developing effective anti-icing strategies for resisting the ice formation and accumulation is an urgent work.[47] Conventional hydrophilic surface tends to induce ice formation due to the adhesion of water, which makes it difficult to achieve anti-icing and deicing. In contrast, solar-to-thermal materials with superhydrophobic surface can effectively reduce droplets adhesion and make them roll away the surface before ice nucleation to anti-icing.[48] Moreover, the presence of an air layer between the micro–nano superhydrophobic structures

Table 1. Performance comparison of SSTMs obtained from different fabricating methods.

Fabricating strategy	Components	Absorptivity	Reflectivity	Temperature (under one sun)	Contact/sliding angle	Features	Stability	Refs.
Laser-etching	PTFE membrane	33.8–68.1% (220–1400 nm)	–	63.2 °C	159.6°/–	High breathability Elasticity	20 times water flushing	[31]
	Copper plates	≈82–95% (300–2500 nm)	–	73.3 °C	155°/10.3°	Robustness Mechanical Durability Icephobic	400 linear abrasion cycles (steel plate)	[32]
Spraying	Cuttlefish juice, SiO_2	70–98% (300–2500 nm)	–	67.6 °C	156.7°/2°	Self-deicing Environmental tolerance Arbitrary substrate	UV irradiation (72 h) Acid–base solution (72 h)	[36]
	WCNTs, beeswax, PDMS	≈99.2% (400–1600 nm)	0.004%	81.6 °C	159.5°/1°	Self-healing Self-cleaning Solar steam generation	Acid–base solution(100 h)	[37]
Template method	Carbon nanopowder, PDMS	≈98.3% (300–2000 nm)	–	75 °C	153.5°/–	Heat transfer Environmentally friendly Anti-icing	Tape peeling (50 cycles) Acid–base solution(10 h) Scratching test (50 cycles)	[38]
Chemical vapor deposition	Carbon soot, silica shell, PDMS	–	<5%	76 °C	163°/–	Self-healing High durability Anti-icing	Icing/deicing (20 cycles)	[39]
Electrochemical deposition	Carbon cloth, pyrrole, 1H,1H,2H,2H-perfluorodecyltrimethoxysilane	≈99% (300–2500 nm)	<1%	90 °C	155°/–	High conversion efficiency Flexibility Anti-icing	Bending–twisting(10 cycles) Abrasion (10 cycles)	[40]
Liquid phase deposition	Polyurethane sponge, Fe_3O_4, poly dopamine	–	–	51 °C (Under −30 °C)	150°/–	Self-cleaning Self-healing Anti-icing	Oxygen plasma etching (12 cycles)	[41]
	Textile, pyrrole, perfluorodecyl triethoxysilane	≈96% (300–2500 nm)	<4%	65 °C	159°/–	Electrothermal conversion Flexibility Stability	Sandpaper abrasion (10 cycles)	[15f]
Dip-coating	Melamine sponge, MXene	11–95% (200–1200 nm)	–	53 °C	151.5°/–	Absorption stability Oil collection Purification	Absorption/deabsorption (10 cycles)	[42]
	Polydopamine, SiO_2, PDMS	–	–	100 °C	163°/–	Thermal management Anti-icing/deicing UV protection	Tape peeling (50 cycles) Ultrasonic treatment (4 h)	[43]
Layer-by-layer assembly	MWCNTs, ethylene-vinyl acetate, n-octadecylamine	–	–	≈63 °C	165°/–	Flexibility Light manipulation Deicing	Droplet impact (1 h) Ethanol immersion (36 h)	[44]

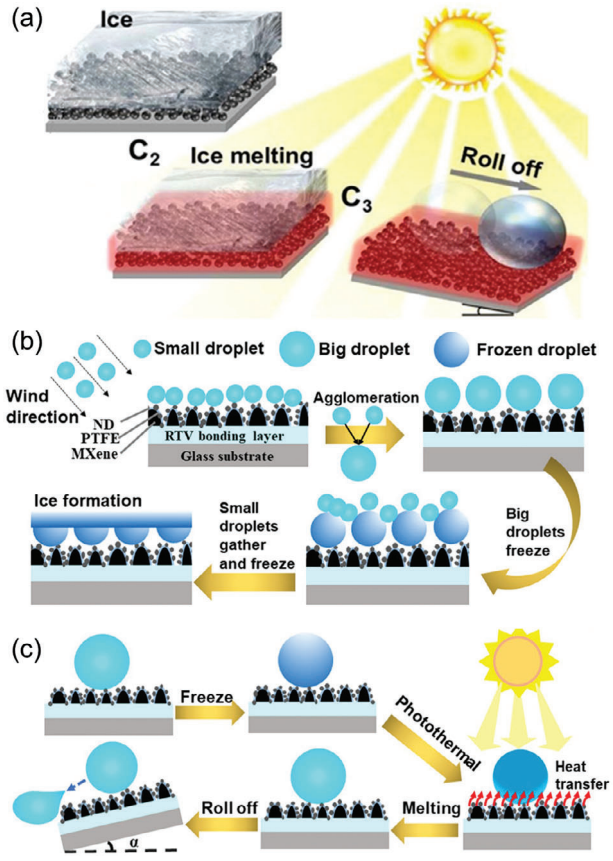

Figure 10. The anti-icing and deicing mechanism of SSTMs. a) Schematic diagram of anti-icing and deicing process of SSTMs. Reproduced with permission.[39] Copyright 2020, National Academy of Sciences. The c) anti-icing and b) deicing mechanism diagrams of SSTMs. Reproduced with permission.[54] Copyright 2022, American Chemical Society.

and droplets hinders heat transfer and delays icing.[49] The photothermal property functions to heat and melt ice, allowing the resulting water droplets to roll away from the targeted surfaces.[27b,50] Both functions cooperate together to achieve high efficiency and continuous anti-ice/de-icing.

As illustrated in **Figure 10a**, a superhydrophobic solar-to-thermal ice-phobic coating was reported, which was composed of three components including candle soot, silicone shell, and polydimethylsiloxane (PDMS) brush. The multilevel micro–nano structures and intrinsic solar-to-thermal capacity of candle soot could trap sunlight in the layered structure and enhance light absorption. At the same time, the silicon dioxide shell and the grafted low surface energy PDMS brush further provided robust superhydrophobic properties. As a result, based on the construction of the robust structures and the synergistic functions, the obtained coatings could accelerate the melting of ice under sunlight, and the melted water droplets tended to spontaneously roll away from the superhydrophobic surface.[39]

The mechanism diagrams of anti-icing and deicing of SSTMs are shown in Figure 10b,c. Under the effect of gravity and wind, small overcooled droplets in the air are easy to fall on the surface of SSTMs and some with initial velocities can bounce away from the superhydrophobic surface;[51] while, others will further aggregate in the growth process. The aggregated large droplets hang on top of the multilevel structures in the Cassie state, and triggered by coalescence, they can gain sufficient kinetic energy to spontaneously depart from the surface in the format of self-propelled jumping.[52] As the bounce and self-jumping behaviours occur before the heterogeneous ice-nucleation, these can reduce the residence time of droplets and will contribute to anti-icing. On the other hand, the air layer with low thermal conductivity is formed between the overcooled large droplets and hierarchical structures, which weakens the heat transfer from the hotter water droplets to the colder superhydrophobic surface and delays the freezing time of droplets at the SSTMs interface (Figure 10b).[53] In addition, the micro–nano structures of the superhydrophobic surface decrease the contact area between the formed ice and the surface, resulting in reduced ice adhesion and improved deicing efficiency. When the sun shines continuously on the surface of SSTMs, the temperature gradually rises due to the solar-to-thermal conversion, resulting in heat absorption and melting of ice. Owing to the limited contact area and adhesion between the ice and the surface, the melted droplets are easy to roll off the inclined superhydrophobic surface (Figure 10c).[54]

Based on the above mechanisms, SSTMs featured with solar-to-thermal properties and water repellency are committed to apply to anti-icing and de-icing. One example developed a carbon-based superhydrophobic solar-to-thermal fabric (ST@CA/CC) utilizing carbon materials with black micro–nano hierarchy structures and photothermal properties.[40] The solar-to-thermal temperature could reach up to 90 °C under one sun, and the superhydrophobic micro–nano structures enhanced the anti-icing performance. Through the dynamic solar-to-thermal deicing experiment on the inclined surface ($\theta = 20°$), it could be clearly observed that after 67 s on solar irradiation, the completely melted frozen droplet rolled away the ST@CA/CC surface, showing the remarkable anti-icing and deicing performance of the obtained fabric (**Figure 11a**). More recently, another example developed a new superhydrophobic solar-to-thermal array with honeycomb wear-resistant structure, which showed a stable melting time of frozen droplets on the surface before and after 200 linear wear cycles. The specific structural design was highly preferred in complex and varied outdoor anti-icing and deicing applications (Figure 11b).[32]

In addition to the good mechanical stability of SSTMs, the challenge of melting ice outdoors cannot be overlooked due to the limited solar irradiation in winter. To address the problem in outdoor applications, a superhydrophobic coating with both solar-to-thermal and electrothermal properties (PESC) is reported, which can achieve anti-icing and deicing at extremely low temperatures throughout the day.[55] On a sunny day, solar energy can be converted into chemical energy stored in the battery, and the coated surface is heated by sunlight to prevent freezing. The power provided by the battery ensures that the deicing coating can work well even on cloudy days or at night (Figure 11c). The efficient all-weather anti-icing and deicing devices show a broad application prospect in the power industry.

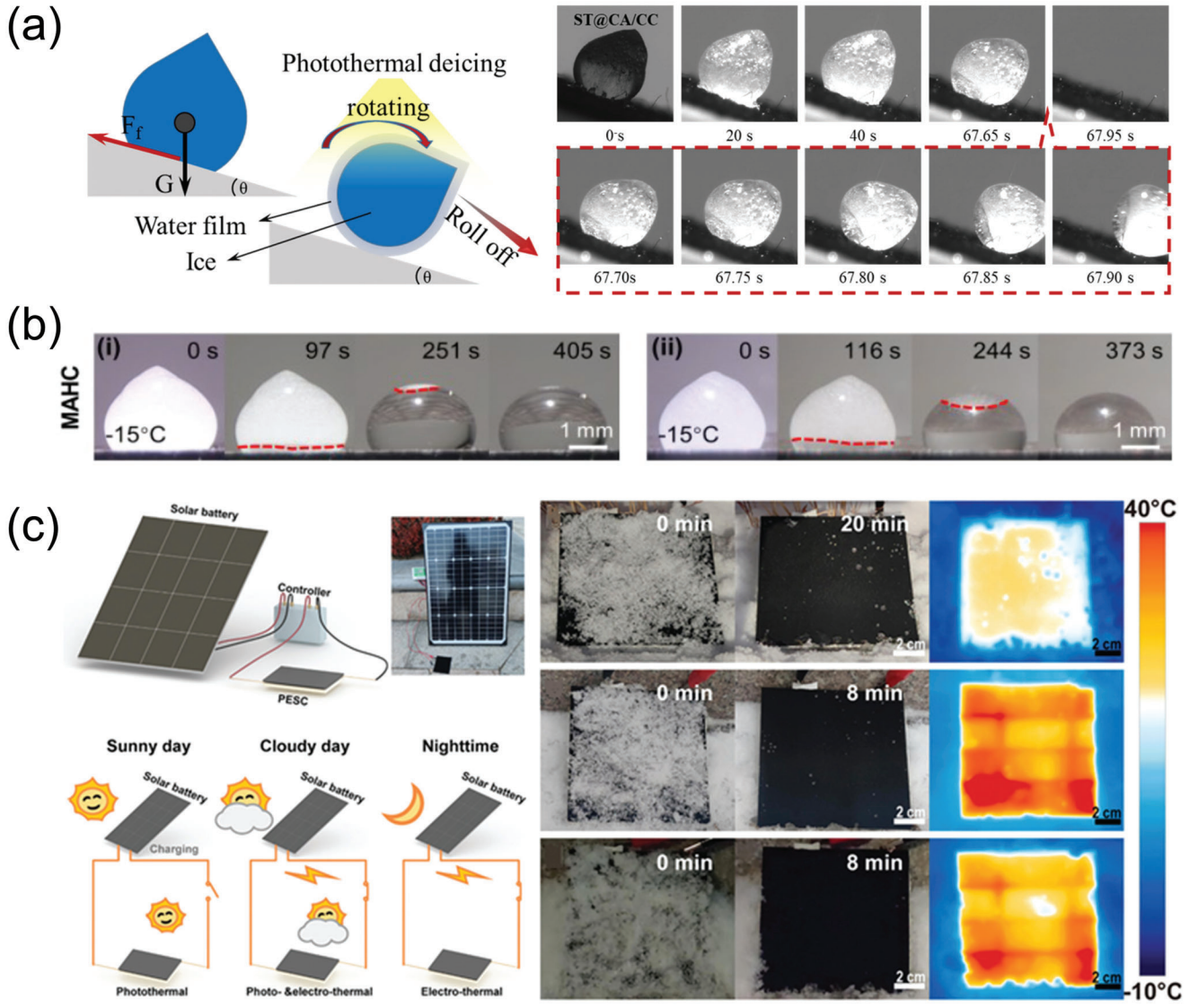

Figure 11. The anti-icing and deicing applications of SSTMs. a) Photothermal deicing process of a freezing droplet on ST@CA/CC. Reproduced with permission.[40] Copyright 2021, American Chemical Society. b) Melting process of a frozen droplet on the robust surfaces b-i) before and b-ii) after 200 linear abrasion cycles under one sun illumination. Adapted with permission.[32] Copyright 2023, John Wiley and Sons. c) Schematic diagrams and anti-icing photographs of self-powered PESC system on the sunny day, cloudy day, and at nighttime outdoor, respectively. Adapted with permission.[55] Copyright 2021, John Wiley and Sons.

4.2. Seawater Desalination

Solar evaporation is an effective strategy of seawater desalination that converts solar energy into thermal energy, which heats at the water–air interface and produces fresh water in designed devices.[56] Photothermal materials with superhydrophilicity can directly transfer the converted thermal energy to the water for evaporation. However, the high salt concentrations and algae pollutants in seawater will block water channels and cover the photothermal surfaces, resulting in low efficiency and discontinuous seawater evaporation.[57] To achieve long-term anti-salt seawater evaporation, SSTMs with water-repellency and self-cleaning are necessary, which can efficiently prevent seawater infiltration and salt blockage and reduce pollutants cover.[33,58] Further, the superhydrophobic micro–nano structures can enhance the sunlight absorption of photothermal materials, thereby improving the photothermal conversion efficiency.

Based on the aforementioned advantages, a commercial polyimide film was first reported by one-step laser treatment, enabling the mass production of carbon-based Janus superhydrophobic/super-hydrophilic porous films.[59] As displayed in **Figure 12a**, compared with other state-of-the-art solar steam generators (e.g., 3D artificial umbrella structured), the graphene film transported water on the super-hydrophilic side and achieved the floating and heating on water surface in the superhydrophobic side, showing the high evaporation efficiency of the 2D film. The principle of anti-salt and pollution resistance of superhydrophobic film is illustrated in Figure 12b. Owing to the

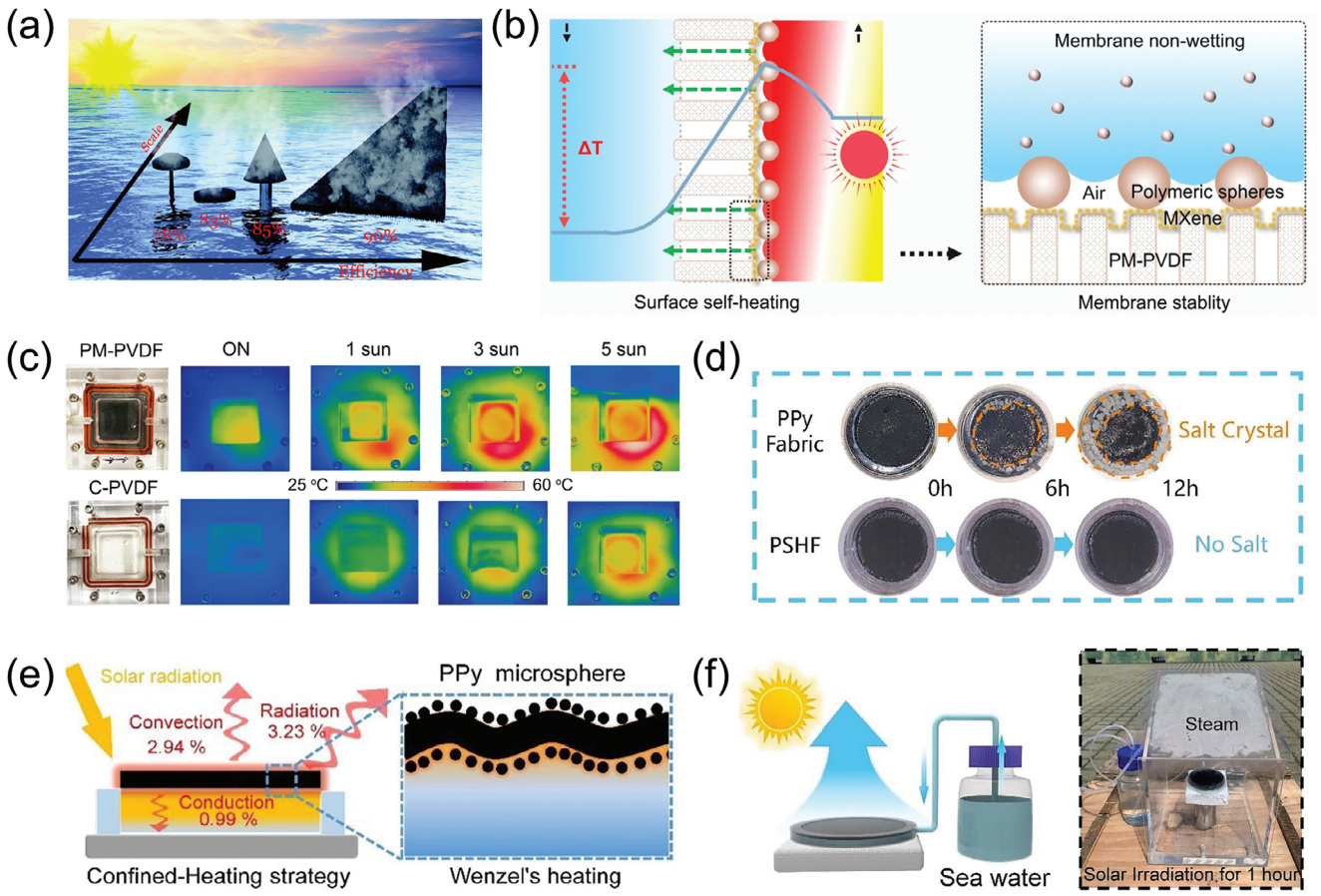

Figure 12. The mechanism and functions of SSTMs for seawater desalination. a) A floating graphene membrane for evaporating seawater using solar energy. Reproduced with permission.[59] Copyright 2018, Royal Society of Chemistry. b) Schematic diagram of the principle of stable heating evaporation and salt resistance of superhydrophobic solar-to-thermal film. c) The infrared images of distillation evaporation between superhydrophobic membrane and conventional membrane under one sun. Reproduced with permission.[60] Copyright 2022, Springer Science and Business Media LLC and Nature Publishing Group. d) Salt resistance and e) superhydrophobic heating principle of the confined-heating system. f) Schematic diagrams of seawater evaporation outdoor in confined-heating system. Reproduced with permission.[15k] Copyright 2022, Elsevier.

solar-to-thermal effect, the local surface is heated with solar irradiation, which ensures the great cross-membrane temperature gradient to heating seawater. As the superhydrophobic polymer particles prevent seawater and salt particles outside, the superhydrophobic solar-to-thermal films show a constant temperature gradient to continuously and stably heat seawater evaporation and salt resistance. As shown in Figure 12c, Wang's group developed a $Ti_3C_2T_x$ MXene-engineered membrane, which improved the local photothermal conversion efficiency and water repellency via alternative spraying of polymer nanospheres and superhydrophobic MXene nanosheets. Superior to conventional infiltrating film, the superhydrophobic solar-to-thermal membrane represented the capability of resisting moisture and further achieving energy-efficient and hypersaline-stable performance in the evaporation process for fresh water yield.[60]

To achieve high efficiency and stable salt-repellent evaporation, our group proposed a solar confined-heating strategy to effectively purify seawater, which could achieve effective salt resistance within 12 h (Figure 12d). The prepared solar-to-thermal and superhydrophobic fabric (PSHF) further integrated onto the top of the additional closed heating device for water circulation through an external pipe.[15k] Compared with the traditional evaporation strategy, the restricted seawater effectively reduced more of the heat loss (7.1%) and achieved better salt resistance, enabling efficient thermal management (Figure 12e). The surface temperature of the PSHF containment strategy could reach up to 59.7 °C, and the evaporation efficiency could reach 91.68% in outdoor experiment (under one sun) (Figure 12f). Although the confined-heating method exhibits high evaporation efficiency, how to design convenient equipment and large-scale seawater desalination on the sea is still a pondered problem for further research.

4.3. Crude Oil Collection

With the sustainable development of the economy and industry, the exploitation and transportation of crude oil leads to frequent oil leakage accidents, which severely impacts the marine environment and ecosystem.[61] Compared to light crude oil, heavy crude oil is difficult to be collected due to its higher viscosity (10^3 to 10^5 mPa at room temperature) and slower diffusion kinetics.

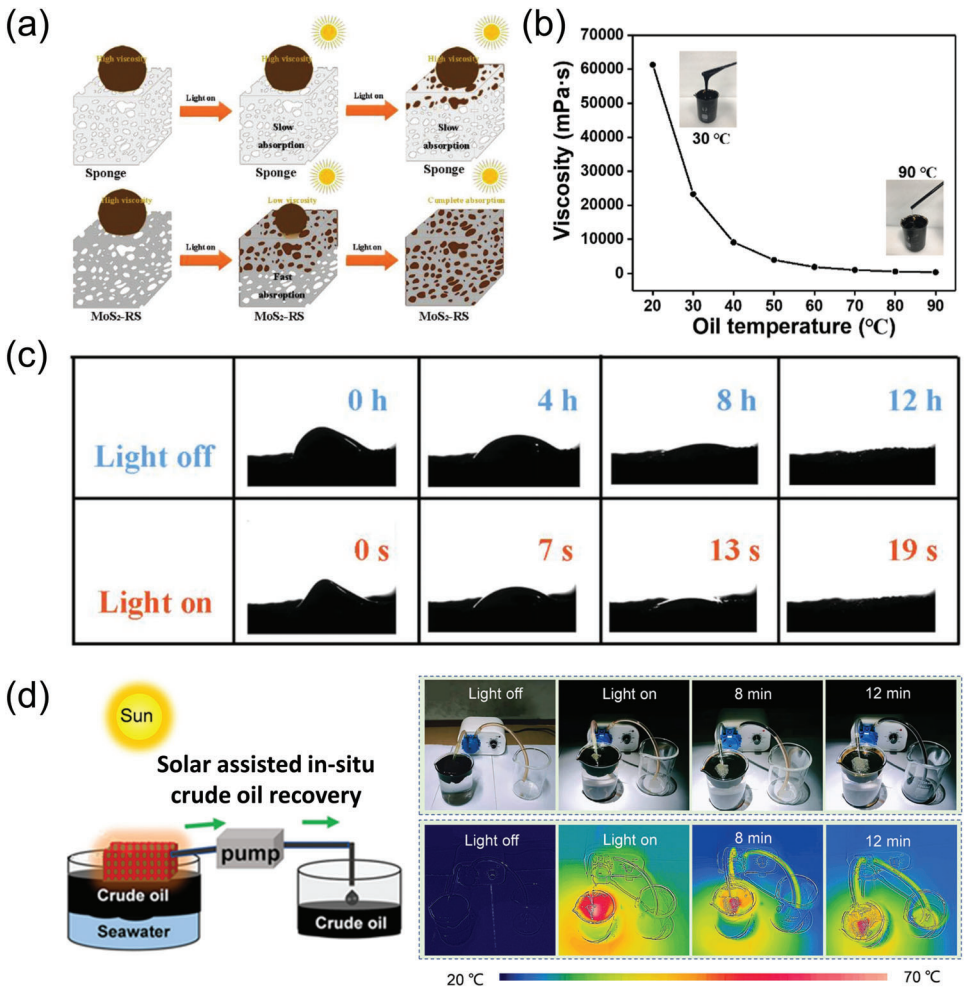

Figure 13. SSTMs for solar assisted crude oil collection. a) The schematic illustration of the crude oil adsorption principles on the unmodified sponge and on superhydrophobic solar-to-thermal sponge under simulated sunlight irradiation. b) The viscosity curve of the crude oil with the temperature increasing. Reproduced with permission.[65] Copyright 2021, Elsevier. c) Photographs of the crude oil adsorption behaviors under dark conditions and with solar irradiation. Adapted with permission.[66] Copyright 2020, John Wiley and Sons. d) The schematic diagram and photographs of continuously collecting the viscous crude oil from the water surface by an in situ pumping device under solar irradiation (1.0 sun). Reproduced with permission.[67] Copyright 2021, American Chemical Society.

Yu's group first introduced a graphene-coated sponge with generated joule heat to improve the adsorption rate of high viscosity crude oil, and further inspired the exploration and research of solar-assisted crude oil technology.[62] As shown in **Figure 13a**, traditional wettability-based adsorption sponges (hydrophobic/lipophilic) fail to capture high viscous leakage oil efficiently due to the low adsorption efficiency and recovery difficulty; while, endowing adsorbent with super-hydrophobicity and solar-to-thermal property is proved to be an effective way to recycle the leaked high viscosity crude oil.[63] Oil–water separation can rely on the water-repellent and lipophilic properties of the superhydrophobic structures to achieve oil absorption, and the photothermal performance of SSTMs converts sunlight into heat to accelerate oil collection and facilitate purification of the absorbed oil.[64]

The crude oil viscosity dramatically decreases with the increased temperature, which is an important inspiration for solving crude oil leakage. An example in Figure 13b indicated that when the temperature of the oil rose from 20 °C to 90 °C, the viscosity of crude oil significantly reduced from 6.1×10^4 to 3.6×10^2 mPa·s. The absorption capacity of crude oil by the superhydrophobic solar-to-thermal sponge increased from 0.84 to 6.14 kg m^{-2}, demonstrating the rapid thermal production on the surface and the fast absorption of crude oil as the temperature of the crude oil rose.[65] The experiments with crude oil adsorption behaviors without or with solar irradiation are shown in Figure 13c. As a control sample, a crude oil droplet was absorbed after 12 h under the dark condition. Once the sunlight was applied, the excellent photothermal effect could accelerate the process within 19 s.[66] Moreover, the superhydrophobic solar-to-thermal sponge was designed as a crude oil collection device, and continuously in situ collected the adsorbed crude oil and pumped under solar irradiation (Figure 13d). It can be clearly observed that the heated crude oil on water surface (red area) was gradually collected by the superhydrophobic solar-to-thermal sponge and pumped to the empty cup nearby. Note that the ingenious design of this device solves the issue of

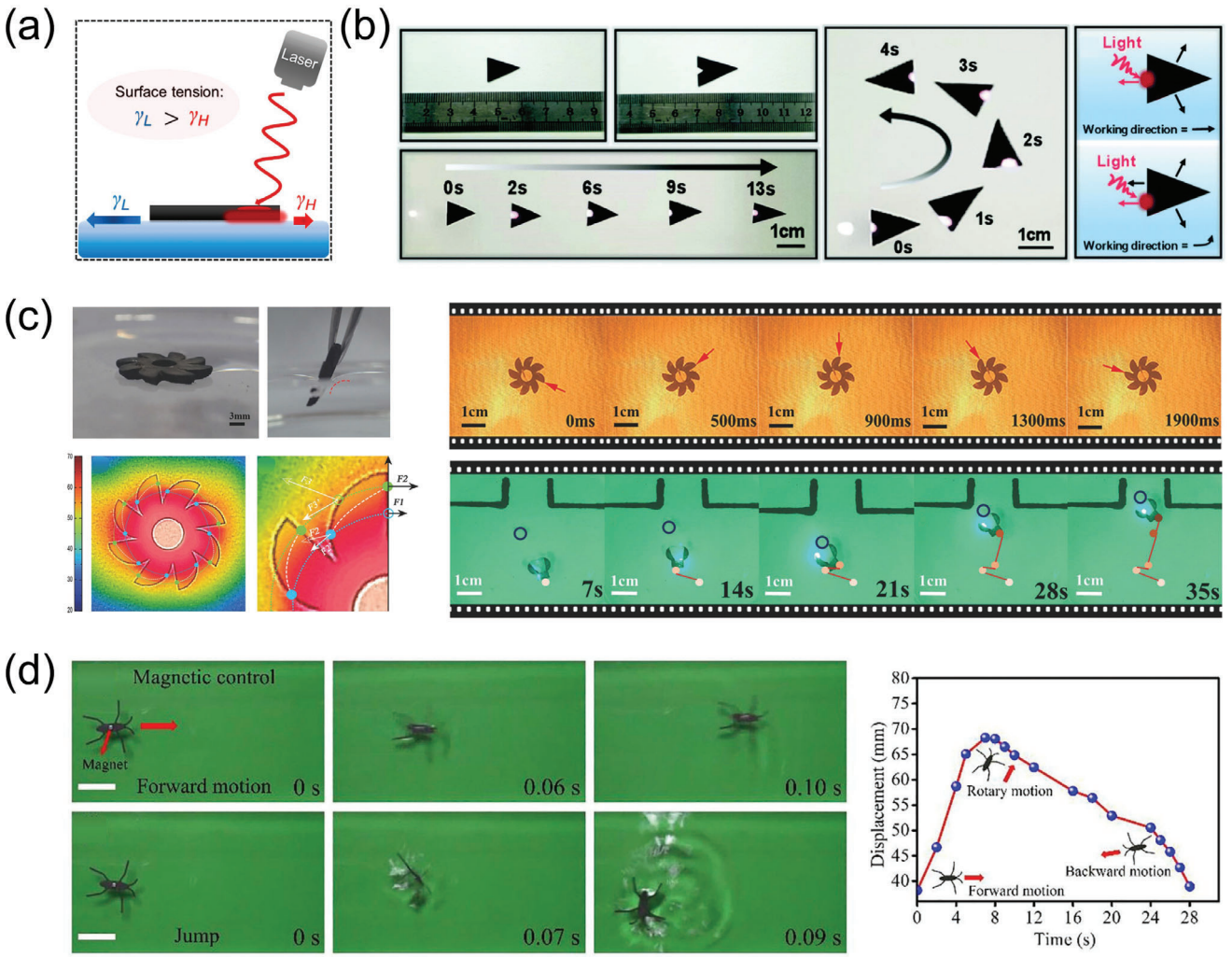

Figure 14. SSTMs as a light-driven actuator and its multimodal motions on water. a) Diagram of water surface induced motion based on the Marangoni effect. Reproduced with permission.[76b] Copyright 2019, American Chemical Society. b) Linear and bending motions of the MXenes-based actuator. Reproduced with permission.[35] Copyright 2019, Royal Society of Chemistry. c) Wetting behaviours of treated PDMS and self-rotational motion of the superhydrophobic floating devices. Adapted with permission.[78] Copyright 2017, John Wiley and Sons. Jumping photographs of the bionic water strider robot (c) and the real-time motion trajectory (d). Reproduced with permission.[68] Copyright 2021, Elsevier.

adsorption saturation and recovery of superhydrophobic solar-to-thermal sponge, showing potential for remediating crude oil leakage.[67]

4.4. Light-Driven Actuators

Autonomous feedback and effective movement strategies allow the water strider to glide effortlessly across the water surface, enabling it to better adapt to a complex and changing living environment.[68] Inspired by this, diverse intelligent multi-response actuators (e.g., heat,[69] light,[15b,70] electricity,[71] magnetic,[72] and moisture[73]) have been developed, which can directly convert various environmental stimuli into mechanical work. Among them, the light-driven strategy for actuators displays broad prospects in environmental protection, micro-robots, and biomedicine due to its advantages of being wireless, remote control enabled, eco-friendly, and controllable.[74]

Surface tension mediated solar-to-thermal superhydrophobic actuator pioneered by Okawa' group, which can directly converse light to work, provides a solution for surface remote controlled actuators.[75] The photothermal performance of SSTMs heats the water through thermal radiation, resulting in a reduction of surface tension. The resulting surface tension gradient promotes the water surface movement of actuators (**Figure 14a**).[76] The superhydrophobic structures and low surface energy of SSTMs can reduce the fluid resistance and enhance solar absorption, causing an increased motion rate of the light-driven actuators.[77] The collaboration of superhydrophobic surface and photothermal conversion enables efficient movement of the actuators.

To demonstrate the advantages of superhydrophobic light-driven actuators, different motion modes are discussed including linear, curve, rotation, and jump. One example of synthetic superhydrophobic surface was reported that introduced hydrophobic multilayers of MXenes on both flexible (e.g., fabric and

paper) and rigid (e.g., glass) substrate, demonstrating the practicability of optical propulsion machines. The prepared 2D MXenes superhydrophobic actuators not only displayed strong resistance to various mechanical damage and chemical corrosion but also realized the linear and bending motions of the triangular actuators on the water surface by adjusting the position of the laser irradiation (Figure 14b).[35] Moreover, a light-driven flotation device featured with light absorption and drag reduction functions via direct laser writing was first fabricated, which could allow for the design of arbitrary patterns and surface modification. The designed asymmetric structure could enable the actuator to achieve self-rotational motion and directional transport object (Figure 14c).[78] This superhydrophobic solar-to-thermal actuator provided a simple, green, and economical preparation method.

Except for light-driven induction, the addition of magnetism can endow the actuator with diverse motion strategies. For instance, the developed graphene/PDMS composite materials can not only achieve a variety of motions such as linear, rotational, and oscillation under infrared light but also realize 180° flip jump (magnetic control) by loading NdFeB magnets on the water strider robot (Figure 14d),[68] which inspires more remote works on water to be achieved, including water environment monitoring and materials transportation.

4.5. Smart Thermal Management

Excessive energy consumption directly leads to global warming and extreme weather.[79] Recently, a variety of thermal management materials has been developed to provide comfortable living conditions for the human body and space, including photothermal films,[80] fabrics,[81] coatings,[82] and hydrogels.[83] However, the conventional solar-to-thermal systems are inevitably exposed to water environment, which will experience a sharp temperature decrease and discontinuous heating performance due to the water's wettability. Benefiting from the capacities of the enhanced light absorption and water repellency, SSTMs with superhydrophobic performance can improve the photothermal conversion efficiency and maintain continuous heating. The photothermal property of SSTMs plays a role in converting sunlight into thermal energy, and further, heating space or human body via thermal radiation. This section predominantly focuses on personal thermal management and indoor thermal management.

Owing to the flexible, comfortable, and washable characteristics, wearable smart textiles have been widely employed for human movement monitoring,[84] medical electronics,[85] electromagnetic interference,[86] personal thermal management,[6b] and other fields. As displayed in **Figure 15**a, a superhydrophobic solar-to-thermal garment that provided thermal energy to the human body under near-infrared irradiation was developed. The functional coating could prevent the fabric wetting by water and maintain the sustaining heating performance.[87] The obtained smart textile exhibited superior solar-to-thermal conversion property (59 °C within 300 s) and water repellency (Figure 15b). Further, the smart textile displayed the property of strain sensing and temperature sensing, which can be further used for integrated wearable devices.[88]

Recently, our group reported a bionic ultra-black textile with ultra-high absorptivity (≈96%) and superhydrophobic capabilities. This textile was demonstrated to the suitable materials used as rescue vests, helping people in danger to float upward from the water and recharge heat for them. From the infrared images in Figure 15c, it was easily observed that the superhydrophobic solar-to-thermal fabric could maintain a continuous and stable surface temperature even in water, showing great potential in multifunctional solar-to-thermal wearable devices.[15f] In another instance, by PDA deposition (solar-to-thermal layer) and spraying PDMS@SiO_2 suspension (low surface energy), a superhydrophobic solar-to-thermal coating with hierarchical micro–nano structures was prepared, which could be quickly heated up to 100 °C under 100 mW cm^{-2} solar irradiation.[43] Compared to the traditional black fabric, the PDMS@SiO_2/PDA fabric displayed better superhydrophobic properties (WCA = 163°) and higher solar-to-thermal conversion efficiency under low solar irradiation (35 mW cm^{-2}) (Figure 15d).

As for indoor thermal management, our group also developed a Janus composite membrane (SPCM), which could achieve the robust interlocked structure by embedding the candle soot component in a transparent elastomer matrix (PDMS).[11] The obtained film showed an efficient sunlight absorption on the PDMS side and significantly enhanced thermal radiation on the carbon side (**Figure 16**a). The good solar-to-thermal property (≈68 °C) and water repellency (≈159.7°) ensured the Janus film further continuously heating indoor space and maintaining temperature stabilization (Figure 16b,c). Further, the Janus film with interlocked structure could be used as a self-sufficient agricultural membrane to effectively promote the growth of bean sprouts, indicating important potential in urban agriculture (Figure 16d). Nevertheless, the trade-off between solar-to-thermal materials and transparency poses a significant challenge for large-scale applications.

4.6. Other Applications

In the past few years, the global economy and human health have been severely affected by the emergence of COVID-19.[89] Disposable medical masks have been identified as an effective measure to control the spread of droplets and ultimately reduce the risk of infection. However, there are certain limitations in existing surgical masks, such as the difficulty to filter bacteria and viruses, the residue of droplets carrying with viruses, and poor sustainability.[90] SSTMs with photothermal and superhydrophobic properties can resolve the above challenges. By the water repellency and self-cleaning of superhydrophobic structures, SSTMs prevent the droplets with virus-carrying from staying on surface and further achieve sterilization through thermal radiation heating of photothermal property (**Figure 17**a).[91] As shown in Figure 17b, the prepared superhydrophobic solar-to-thermal mask can be worn easily owing to the secondary processing on the traditional mask.[92] Further, the SWCNTs superhydrophobic layer (CA ≈ 156.2°) on a melt-blown polypropylene (PP) surgical mask is fabricated by spray-coating technique, which allows the virus-carrying droplets to roll off the mask (Figure 17c).[93] The CNTs-coated mask can also achieve a high temperature of 91.4 °C under one sun which can kill bacteria and virus on mask (Figure 17d**)**. As demonstrated in Figure 17e, *Escherichia coli* ATCC 25922 on CNTs-coated masks shows obvious antibacterial

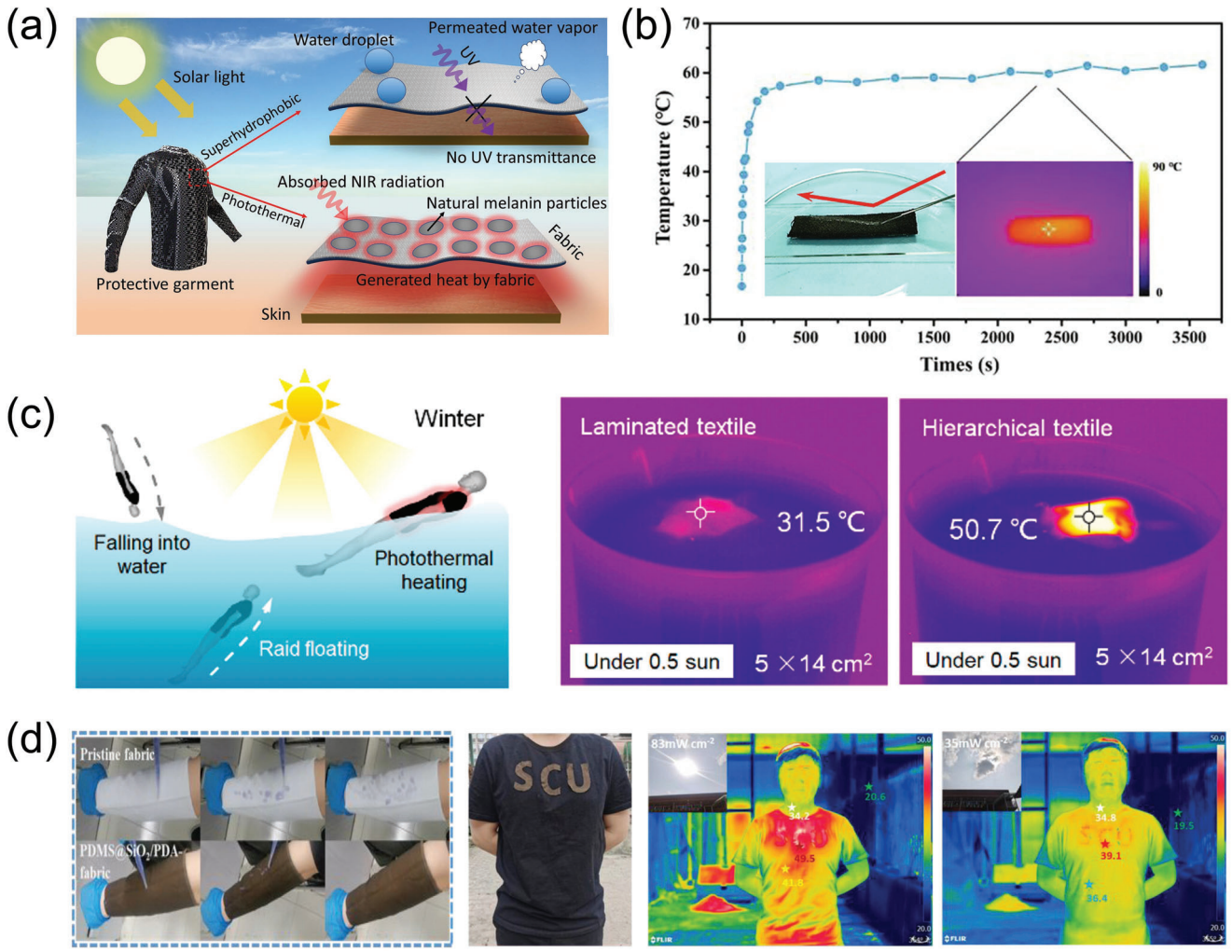

Figure 15. SSTMs for wearable thermal management devices. a) Schematic illustration of novel functionalities of cotton fabric featured with superhydrophobic and solar-to-thermal properties. Reproduced with permission.[87] Copyright 2022, Elsevier. b) Superhydrophobic solar-to-thermal diagram, temperature curve, and water repellent (inset) of functional fabric. Reproduced with permission.[88] Copyright 2021, Elsevier. c) The water rescue diagram and the corresponding temperature of rescue vest under low sunlight irradiation (0.5 sun). Reproduced with permission.[15f] Copyright 2022, American Chemical Society. d) The photographs and infrared images of superhydrophobic solar-to-thermal coating with water repellency and solar-to-thermal performances. Reproduced with permission.[43] Copyright 2023, American Chemical Society.

activity under the mode of solar irradiation (one sun within 1 min); while, the number of *E. coli* in traditional masks does not change. The high-resolution confocal fluorescence images present the additional proof that the coated CNTs mask can eradicate a number of bacteria due to the photothermal conversion (the red area). As the spray-coating method is easily scalable, the CNTs-coated masks are expected to provide solutions for the treatment and prevention of major epidemic.

Last but not the least, based on our previous work, the superhydrophobic solar-to-thermal strategy can be easily incorporated into self-supported sensors to resist the impact of water and sweat. To realize multifunctional sensors, we proposed a method of self-assembly at water/air interface combined with spraying to achieve a superhydrophobic PDMS/CNTs/PDMS sensing membrane (PCPM) with solar-to-thermal conversion.[94] The PCPM could be further designed to construct a smart umbrella with water repellency for monitoring sunlight intensity and weather conditions throughout the day (sunny or rainy) (Figure 17f).

5. Conclusion and Perspective

Based on extensive advances on SSTMs, the structural combination of superhydrophobic and solar-to-thermal surfaces with synergistic functions has been manufactured and applied in emerging fields of icing/melting resistance, solar evaporation, light-driven actuation, crude oil collection, antibacterial surfaces, and wearable/outdoor thermal management. The alternative introduction of superhydrophobic micro–nano structures and functions into the photothermal materials has been proved to remarkably promote the efficiency and stability of solar-to-thermal conversion. In this review, we first introduce the construction mechanism and functions of SSTMs. Further, a series of typical construction strategies of laser-etching, spraying, dip-coating,

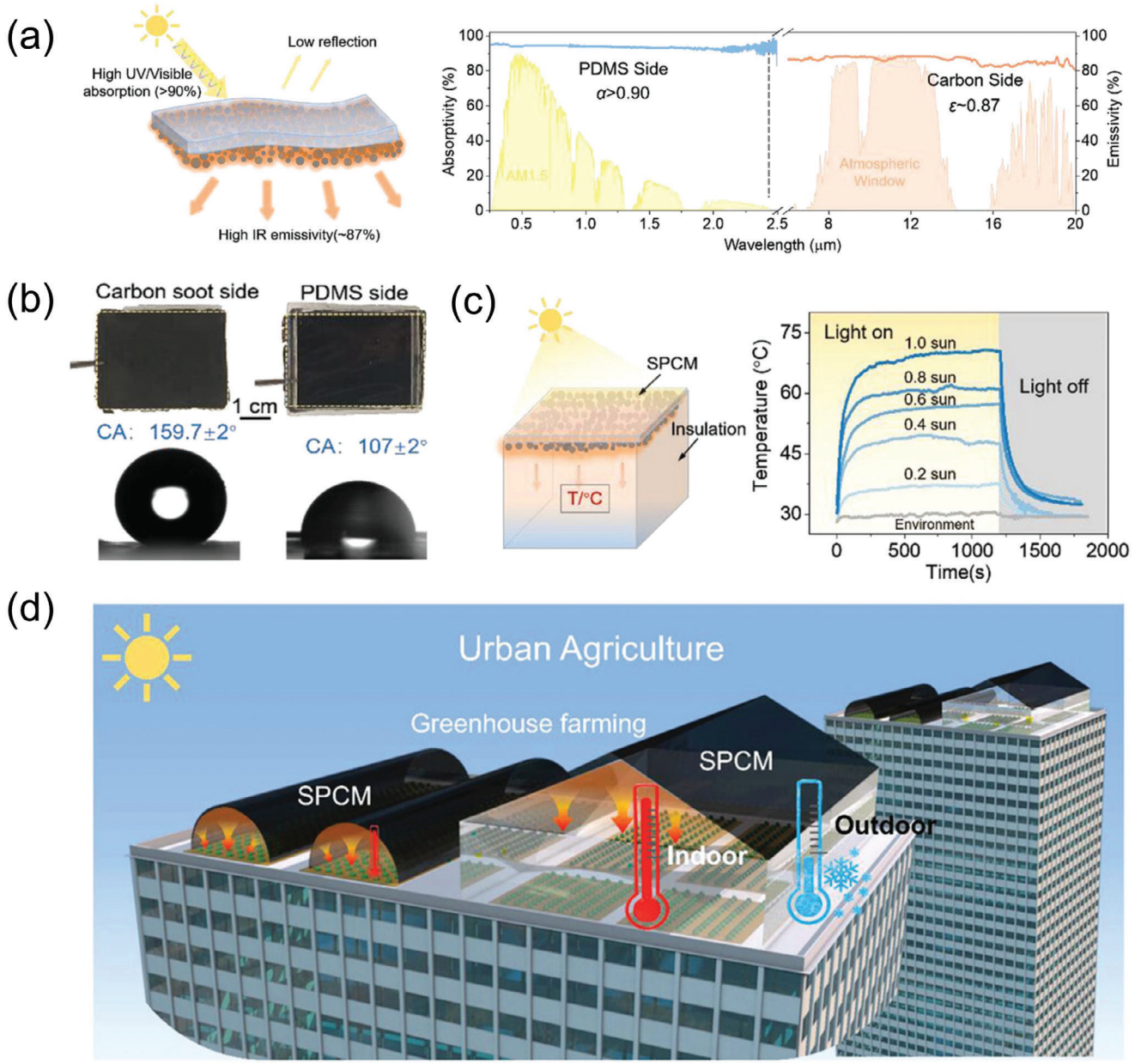

Figure 16. SSTMs thermal management for urban agriculture. a) Working mechanism and optical property diagrams of SPCM. b) Superhydrophobic characteristics and c) thermal management capability under different sunlight intensities of SPCM. d) Potential application of SPCM in urban agriculture. Adapted with permission.[11] Copyright 2023, John Wiley and Sons.

chemical deposition, layer-by-layer assembly, and also their pros and cons are described in detail. Finally, the cutting-edge and blooming applications of SSTM are sufficiently discussed, which aim to realize high-efficiency and stable conversion and utilization of solar energy.

Despite significant progress in SSTMs, several pressing challenges still remain to be addressed in practical applications. First, the mechanical stability and environmental durability of SSTMs should be further improved. The conventional micro–nano structures of superhydrophobic surfaces are easily destroyed by mechanical abrasion. Some typical examples of the rain erosion, fabric friction, and joint tension have proposed high requirements for the mechanical stability of SSTMs. Once the superhydrophobic micro–nano surface is destructed, macroscopic water droplets with high specific heat capacity and heat dissipation can quickly form a wetted interface with the destroyed surface, resulting in severe degradation of photothermal efficiency. In addition, the size of micro–nanostructures can remarkably affect the wettability of superhydrophobic surface, especially under extreme environments (e.g., low temperature and high humidity), which needs further theoretical research and structural design to enhance extreme environment tolerance. In addition, SSTMs that

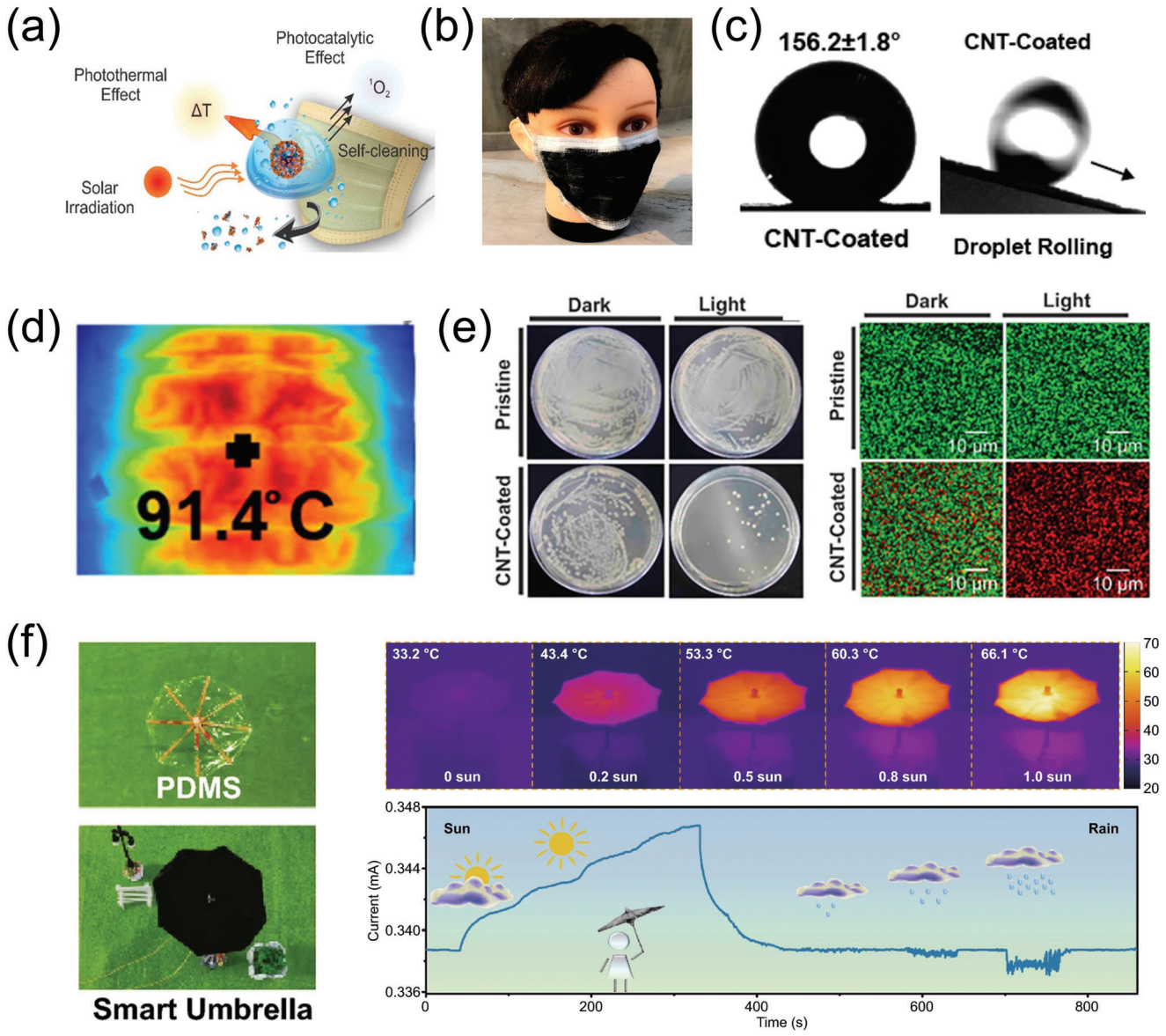

Figure 17. SSTMs for antibacterial masks and multifunctional devices. a) Schematic diagram of mask hydrophobic self-cleaning and photothermal sterilization under solar irradiation. Reproduced with permission.[91c] Copyright 2021, American Chemical Society. b) Photograph of the laser-fabricated graphene mask. Reproduced with permission.[92] Copyright 2020, American Chemical Society. c) Water contact angle images and d) infrared image of the CNTs-coated mask under one sun. e) The antibacterial photographs and confocal fluorescence images of *E. coli* ATCC 25922 under solar illuminated and dark conditions. Reproduced with permission.[93] Copyright 2021, American Chemical Society. f) Infrared images of the smart umbrella under different solar intensity and the intelligent monitoring of weather conditions throughout the day. Reproduced with permission.[94] Copyright 2021, The Author(s).

are applicable to diverse nonplanar surfaces should be further developed. Commonly, the current construction approaches of SSTMs are based on flat substrates. For typical applications on macroscopically rough and even 3D curved surfaces, it is difficult to adapt for SSTMs. Moreover, conventional superhydrophobic photothermal materials featured with high light absorptivity and rough micro–nano structured surfaces are generally opaque or black, which severely limits their further application fields, especially in automotive windshields, solar panel and optics, smart windows, and related energy-saving building systems. Considering the environmental and biological toxicity, the widely used fluorophobic agents that can remarkably reduce the surface energy should also be replaced by other environmentally friendly alternative materials (e.g., paraffin, fatty acids, and proteins) or hydrophobic chemical groups of alkyls. Finally, some simple, high-efficient, and cost-effective fabrication strategies with the capability of scalable production should be considered for practical applications, ensuring the achievement of large-scale and highly uniform SSTMs.

Nowadays, the development and exploration of SSTMs are still in the infancy. However, the blooming SSTMs system with synergetic functions show unique performance and significant potentials in widespread fields of anti-icing functional surfaces, sustainable water purification, crude oil collection, solar-driven soft

actuation, wearable/outdoor thermal management, and so on. We believe that many research fields, especially some crossing ones, can benefit a lot from this review, which will also inspire new structural design of SSTMs system and extendable novel applications.

Acknowledgements

This project was financially supported by the Natural Science Foundation of China (52373094, 52073295), the Ningbo Science and Technology Bureau (2021Z127), the Sino-German Mobility Program (M-0424), and the Ningbo Public Welfare Science and Technology Plan Project (2021S150).

Conflict of Interest

The authors declare no conflict of interest.

Keywords

photothermal materials, solar-to-thermal conversion, superhydrophobic surface, synergetic functions, thermal management applications

Received: October 31, 2023
Revised: April 30, 2024
Published online:

[1] a) N. Kannan, D. Vakeesan, *Renewable Sustainable Energy Rev.* **2016**, *62*, 1092; b) N. S. Lewis, *Science* **2007**, *315*, 798; c) L. Zhu, M. Gao, C. K. N. Peh, G. W. Ho, *Mater. Horiz.* **2018**, *5*, 323; d) K. Khaletskaya, J. Reboul, M. Meilikhov, M. Nakahama, S. Diring, M. Tsujimoto, S. Isoda, F. Kim, K.-i. Kamei, R. A. Fischer, S. Kitagawa, S. Furukawa, *J. Am. Chem. Soc.* **2013**, *135*, 10998; e) M. S. Yavuz, Y. Cheng, J. Chen, C. M. Cobley, Q. Zhang, M. Rycenga, J. Xie, C. Kim, K. H. Song, A. G. Schwartz, L. V. Wang, Y. Xia, *Nat. Mater.* **2009**, *8*, 935; f) Statistical Review of World Energy 2021. *Steel Scenario* **2021**, *10*; g) S. Shafiee, E. Topal, *Energy Policy* **2009**, *37*, 181; h) M. Liao, W. Xu, Y. Song, Z. Pan, H. Zheng, Y. Li, X. Qin, L. Wang, J. Lu, Z. Wang, *Nano Energy* **2023**, *116*, 108831.

[2] a) M. L. Brongersma, N. J. Halas, P. Nordlander, *Nat. Nanotechnol.* **2015**, *10*, 25; b) T. D. Y. Kozai, A. L. Vazquez, *J. Mater. Chem. B* **2015**, *3*, 4965; c) K.-T. Lin, H. Lin, T. Yang, B. Jia, *Nat. Commun.* **2020**, *11*, 1389; d) X. Wang, Q. Liu, S. Wu, B. Xu, H. Xu, *Adv. Mater.* **2019**, *31*, 1807716; e) P. Xiao, J. He, F. Ni, C. Zhang, Y. Liang, W. Zhou, J. Gu, J. Xia, S.-W. Kuo, T. Chen, *Nano Energy* **2020**, *68*, 104385.

[3] a) F. Zhang, D. Xu, D. Zhang, L. Ma, J. Wang, Y. Huang, M. Chen, H. Qian, X. Li, *Chem. Eng. J.* **2021**, *423*, 130238; b) H. Liu, G. Huang, R. Wang, L. Huang, H. Wang, Y. Hu, G. Cong, F. Bao, M. Xu, C. Zhu, J. Xu, M. Ji, *ACS Appl. Mater. Interfaces* **2022**, *14*, 32404; c) S. Huang, H. Liu, K. Liao, Q. Hu, R. Guo, K. Deng, *ACS Appl. Mater. Interfaces* **2020**, *12*, 28952.

[4] a) X. Wu, S. Cao, D. Ghim, Q. Jiang, S. Singamaneni, Y.-S. Jun, *Nano Energy* **2021**, *79*, 105353; b) R. Li, G. Zhang, L. Yang, C. Zhou, *Sep. Purif. Technol.* **2021**, *276*, 119372; c) Q. Zhao, Y. Wan, F. Chang, Y. Wang, H. Jiang, L. Jiang, X. Zhang, N. Ma, *Desalination* **2022**, *527*, 115581; d) P. Cheng, D. Wang, P. Schaaf, *Adv. Sustainable Syst.* **2022**, *6*, 2200115.

[5] G. Guan, K. Y. Win, X. Yao, W. Yang, M.-Y. Han, *Adv. Healthcare Mater.* **2021**, *10*, 2001158.

[6] a) Z. Chen, L. Dong, D. Yang, H. Lu, *Adv. Mater.* **2013**, *25*, 5352; b) Y. Peng, Y. Cui, *Joule* **2020**, *4*, 724; c) F. L. Zhu, Q. Q. Feng, *Int. J. Therm. Sci.* **2021**, *165*, 106899.

[7] a) E. Celia, T. Darmanin, E. Taffin de Givenchy, S. Amigoni, F. Guittard, *J. Colloid Interface Sci.* **2013**, *402*, 1; b) A. Elzaabalawy, S. A. Meguid, *Int. J. Mech. Mater. Des.* **2022**, *18*, 509; c) N. J. Shirtcliffe, G. McHale, S. Atherton, M. I. Newton, *Adv. Colloid Interface Sci.* **2010**, *161*, 124; d) Y. Y. Yan, N. Gao, W. Barthlott, *Adv. Colloid Interface Sci.* **2011**, *169*, 80; e) Y. Jin, C. Wu, P. Sun, M. Wang, M. Cui, C. Zhang, Z. Wang, *Droplet* **2022**, *1*, 92.

[8] a) D. Li, L. Ma, B. Zhang, S. Chen, *Chem. Eng. J.* **2022**, *450*, 138429; b) Y. Sun, Y. Wang, W. Liang, L. He, F. Wang, D. Zhu, H. Zhao, *ACS Appl. Mater. Interfaces* **2022**, *14*, 49352; c) S. Wu, Z. Liang, Y. Li, S. Chay, Z. He, S. Tan, J. Wang, X. Zhu, X. He, *Adv. Sci.* **2022**, *9*, 2105986; d) T. Wu, W. Xu, X. Li, Y. Du, M. Sheng, H. Zhong, H. Xie, J. Qu, *ACS Nano* **2022**, *16*, 16624.

[9] a) H. Xie, W. H. Xu, Y. Du, J. Gong, R. Niu, T. Wu, J. P. Qu, *Small* **2022**, *18*, 2200175; b) E. Li, Y. Pan, C. Wang, C. Liu, C. Shen, C. Pan, X. Liu, *ACS Appl. Mater. Interfaces* **2021**, *13*, 28996.

[10] a) S. Tang, Z. Wu, G. Feng, L. Wei, J. Weng, E. Ruiz-Hitzky, X. Wang, *Chem. Eng. J.* **2023**, *454*, 140457; b) H. Wu, J. Luo, X. Huang, L. Wang, Z. Guo, J. Liang, S. Zhang, H. Xue, J. Gao, *J. Colloid Interface Sci.* **2021**, *603*, 282; c) M. K. Fu, I. Arenas, S. Leonardi, M. Hultmark, *J. Fluid Mech.* **2017**, *824*, 688; d) S. Türk, G. Daschiel, A. Stroh, Y. Hasegawa, B. Frohnapfel, *J. Fluid Mech.* **2014**, *747*, 186.

[11] S. Li, P. Xiao, W. Yang, C. Zhang, J. Gu, S. W. Kuo, T. Chen, *Adv. Funct. Mater.* **2023**, *33*, 2209654.

[12] a) Z. Lin, Z. Wang, X. Zhang, D. Diao, *Nano Res.* **2020**, *14*, 1110; b) K. Pal, G. Z. Kyzas, S. Kralj, F. Gomes de Souza, *J. Mol. Struct.* **2021**, *1233*, 130100; c) N. S. Fuzil, N. H. Othman, N. H. Alias, F. Marpani, M. H. D. Othman, A. F. Ismail, W. J. Lau, K. Li, T. D. Kusworo, I. Ichinose, M. M. A. Shirazi, *Desalination* **2021**, *517*, 115259; d) K. Li, T. H. Chang, Z. Li, H. Yang, F. Fu, T. Li, J. S. Ho, P. Y. Chen, *Adv. Energy Mater.* **2019**, *9*, 1901687.

[13] a) A. Elzaabalawy, S. A. Meguid, *Int. J. Mech. Mater. Des.* **2022**, *18*, 509; b) L. Fei, Z. He, J. D. LaCoste, T. H. Nguyen, Y. Sun, *Chem. Rec.* **2020**, *20*, 1257; c) J. Jeevahan, M. Chandrasekaran, G. Britto Joseph, R. B. Durairaj, G. Mageshwaran, *J. Coat. Technol. Res.* **2018**, *15*, 231; d) S. G. Moghadam, H. Parsimehr, A. Ehsani, *Adv. Colloid Interface Sci.* **2021**, *290*, 102397; e) D. Wang, Q. Sun, M. J. Hokkanen, C. Zhang, F.-Y. Lin, Q. Liu, S.-P. Zhu, T. Zhou, Q. Chang, B. He, Q. Zhou, L. Chen, Z. Wang, R. H. A. Ras, X. Deng, *Nature* **2020**, *582*, 55; f) S. Xu, Q. Wang, N. Wang, *Adv. Eng. Mater.* **2021**, *23*, 2001083.

[14] a) C. Chen, Y. Kuang, L. Hu, *Joule* **2019**, *3*, 683; b) X. Cui, Q. Ruan, X. Zhuo, X. Xia, J. Hu, R. Fu, Y. Li, J. Wang, H. Xu, *Chem. Rev.* **2023**, *123*, 6891; c) N. S. Fuzil, N. H. Othman, N. H. Alias, F. Marpani, M. H. D. Othman, A. F. Ismail, W. J. Lau, K. Li, T. D. Kusworo, I. Ichinose, M. M. A. Shirazi, *Desalination* **2021**, *517*, 115259; d) M. Gao, L. Zhu, C. K. Peh, G. W. Ho, *Energy Environ. Sci.* **2019**, *12*, 841; e) L. Xiao, X. Chen, X. Yang, J. Sun, J. Geng, *ACS Appl. Polym. Mater.* **2020**, *2*, 4273; f) P. Zhang, H. Wang, J. Wang, Z. Ji, L. Qu, *Adv. Mater.* **2024**, *36*, 2303976; g) L. Zhu, L. Tian, S. Jiang, L. Han, Y. Liang, Q. Li, S. Chen, *Chem. Soc. Rev.* **2023**, *52*, 7389.

[15] a) F. Ni, P. Xiao, N. Qiu, C. Zhang, Y. Liang, J. Gu, J. Xia, Z. Zeng, L. Wang, Q. Xue, T. Chen, *Nano Energy* **2020**, *68*, 104311; b) S. Wang, Y. Gao, A. Wei, P. Xiao, Y. Liang, W. Lu, C. Chen, C. Zhang, G. Yang, H. Yao, T. Chen, *Nat. Commun.* **2020**, *11*, 4359; c) P. Xiao, J. Gu, C. Zhang, F. Ni, Y. Liang, J. He, L. Zhang, J. Ouyang, S.-W. Kuo, T. Chen, *Nano Energy* **2019**, *65*, 104002; d) P. Xiao, J. He, Y. Liang, C. Zhang, J. Gu, J. Zhang, Y. Huang, S.-W. Kuo, T. Chen, *Sol. RRL* **2019**, *3*, 1900004; e) P. Xiao, J. He, F. Ni, C. Zhang, Y. Liang, W. Zhou, J. Gu, J. Xia, S.-W. Kuo, T. Chen, *Nano Energy* **2020**, *68*, 104385; f) P. Xiao, W. Yang, N. Qiu, S. Li, F. Ni, C. Zhang, J. Gu, S.-W. Kuo, T. Chen, *Nano Lett.* **2022**, *22*, 9343; g) W. Yang, P. Xiao, S. Li, F. Deng, F. Ni, C. Zhang, J. Gu, J. Yang, S. W. Kuo, F. Geng, T. Chen, *Small* **2023**, *19*, 2302509; h) W. Yang, P. Xiao, F. Ni, C. Zhang, J. Gu, S.-W. Kuo, Q. Liu, T. Chen, *Nano Energy* **2022**, *97*, 107180; i) C. Zhang, P. Xiao, F. Ni, L. Yan, Q. Liu, D. Zhang, J. Gu, W. Wang, T. Chen, *ACS Sustainable Chem. Eng.* **2020**,

8, 5328; j) C. Zhang, P. Xiao, F. Ni, Y. Yang, J. Gu, L. Zhang, J. Xia, Y. Huang, W. Wang, T. Chen, *Energy Technol.* **2019**, *7*, 1900787; k) C. Zhang, P. Xiao, F. Ni, J. Gu, J. Chen, Y. Nie, S.-W. Kuo, T. Chen, *Chem. Eng. J.* **2022**, *428*, 131142.
[16] C. G. Granqvist, *Adv. Mater.* **2003**, *15*, 1789.
[17] L. Zhu, L. Tian, S. Jiang, L. Han, Y. Liang, Q. Li, S. Chen, *Chem. Soc. Rev.* **2023**, *52*, 7389.
[18] P. Xiao, W. Yang, N. Qiu, S. Li, F. Ni, C. Zhang, J. Gu, S. W. Kuo, T. Chen, *Nano Lett.* **2022**, *22*, 9343.
[19] J. Wang, Y. Li, L. Deng, N. Wei, Y. Weng, S. Dong, D. Qi, J. Qiu, X. Chen, T. Wu, *Adv. Mater.* **2017**, *29*, 1603730.
[20] C. Zhang, H.-Q. Liang, Z.-K. Xu, Z. Wang, *Adv. Sci.* **2019**, *6*, 1900883.
[21] T. Young, *Philos. Trans. R. Soc. London* **1805**, *95*, 65.
[22] R. N. Wenzel, *Ind. Eng. Chem.* **1936**, *28*, 988.
[23] A. B. D. Cassie, S. Baxter, *Trans. Faraday Soc.* **1944**, *40*, 546.
[24] a) H. Zhou, T. Zhang, X. Yue, Y. Peng, F. Qiu, D. Yang, *Ind. Eng. Chem. Res.* **2019**, *58*, 4844; b) M. J. Nine, M. A. Cole, L. Johnson, D. N. Tran, D. Losic, *ACS Appl. Mater. Interfaces* **2015**, *7*, 28482.
[25] F. Zhang, H. Yan, M. Chen, *Small* **2024**, 2312226, https://doi.org/10.1002/smll.202312226.
[26] a) E. J. Falde, S. T. Yohe, Y. L. Colson, M. W. Grinstaff, *Biomaterials* **2016**, *104*, 87; b) S. Shin, J. Seo, H. Han, S. Kang, H. Kim, T. Lee, *Materials* **2016**, *9*, 116.
[27] a) Y. Wu, L. Dong, X. Shu, Y. Yang, P. Feng, Q. Ran, *Chem. Eng. J.* **2023**, *469*, 143924; b) Q. Cong, X. Qin, T. Chen, J. Jin, C. Liu, M. Wang, *Materials* **2023**, *16*, 5151; c) X. Wu, G. Y. Chen, G. Owens, D. Chu, H. Xu, *Mater. Today Energy* **2019**, *12*, 277.
[28] a) D. Gong, J. Long, P. Fan, D. Jiang, H. Zhang, M. Zhong, *Appl. Surf. Sci.* **2015**, *331*, 437; b) D. K. Sarkar, M. Farzaneh, R. W. Paynter, *Mater. Lett.* **2008**, *62*, 1226.
[29] a) W. Zhao, L. Xiao, X. He, Z. Cui, J. Fang, C. Zhang, X. Li, G. Li, L. Zhong, Y. Zhang, *Opt. Laser Technol.* **2021**, *141*, 107115; b) S. Yang, K. Yin, D. Chu, J. He, J.-A. Duan, *Appl. Phys. Lett.* **2018**, *113*, 203701.
[30] Y. Lin, H. Chen, G. Wang, A. Liu, *Coatings* **2018**, *8*, 208.
[31] Z. Wu, J. Wu, L. Wang, Y. He, T. Wu, Z. Zhu, K. Yin, *Opt. Laser Technol.* **2022**, *152*, 108171.
[32] M. Zhou, L. Zhang, L. Zhong, M. Chen, L. Zhu, T. Zhang, *Adv. Mater.* **2023**, *36*, 2305322.
[33] C. Shen, Y. Zhu, X. Xiao, X. Xu, X. Chen, G. Xu, *ACS Appl. Mater. Interfaces* **2020**, *12*, 35142.
[34] J. Wan, J. Xu, S. Zhu, B. Wang, J. Li, G. Ying, K. Chen, *J. Colloid Interface Sci.* **2023**, *629*, 581.
[35] W.-T. Cao, W. Feng, Y.-Y. Jiang, C. Ma, Z.-F. Zhou, M.-G. Ma, Y. Chen, F. Chen, *Mater. Horiz.* **2019**, *6*, 1057.
[36] C.-H. Xue, H.-G. Li, X.-J. Guo, Y.-R. Ding, B.-Y. Liu, Q.-F. An, Y. Zhou, *Chem. Eng. J.* **2021**, *424*, 130553.
[37] D. Weng, F. Xu, X. Li, Y. Li, J. Sun, *J. Mater. Chem. A* **2018**, *6*, 24441.
[38] Z. Xie, H. Wang, Q. Deng, Y. Tian, Y. Shao, R. Chen, X. Zhu, Q. Liao, *J. Phys. Chem. Lett.* **2022**, *13*, 10237.
[39] S. Wu, Y. Du, Y. Alsaid, D. Wu, M. Hua, Y. Yan, B. Yao, Y. Ma, X. Zhu, X. He, *Proc. Natl. Acad. Sci. U. S. A.* **2020**, *117*, 11240.
[40] Z. Xie, H. Wang, Y. Geng, M. Li, Q. Deng, Y. Tian, R. Chen, X. Zhu, Q. Liao, *ACS Appl. Mater. Interfaces* **2021**, *13*, 48308.
[41] B. Yu, Z. Sun, Y. Liu, Y. Wu, F. Zhou, *Langmuir* **2023**, *39*, 1686.
[42] M. Wang, J. Zhu, Y. Zi, W. Huang, *ACS Appl. Mater. Interfaces* **2021**, *13*, 47302.
[43] Z. Zhao, Q. Zhang, X. Song, J. Chen, Y. Ding, H. Wu, S. Guo, *ACS Appl. Mater. Interfaces* **2023**, *15*, 3522.
[44] X. Su, H. Li, X. Lai, Z. Yang, Z. Chen, W. Wu, X. Zeng, *J. Mater. Chem. A* **2018**, *6*, 16910.
[45] A. K. Menon, I. Haechler, S. Kaur, S. Lubner, R. S. Prasher, *Nat. Sustainability* **2020**, *3*, 144.
[46] X. Tian, T. Verho, R. H. A. Ras, *Science* **2016**, *352*, 142.
[47] a) S. G. Cober, G. A. Isaac, *J. Appl. Meteorol. Climatol.* **2013**, *52*, 1673; b) T. Wang, Y. Zheng, A.-R. O. Raji, Y. Li, W. K. A. Sikkema, J. M. Tour, *ACS Appl. Mater. Interfaces* **2016**, *8*, 14169; c) S. Farhadi, M. Farzaneh, S. A. Kulinich, *Appl. Surf. Sci.* **2011**, *257*, 6264; d) L. Wang, Q. Gong, S. Zhan, L. Jiang, Y. Zheng, *Adv. Mater.* **2016**, *28*, 7729; e) R. Pan, H. Zhang, M. Zhong, *ACS Appl. Mater. Interfaces* **2021**, *13*, 1743; f) S. Yang, Y. Ying, W. Li, Y. Feng, R. Wen, Q. Li, Y. Liu, B. Du, Z. Wang, X. Ma, *Chem. Eng. J.* **2023**, *465*, 142991.
[48] a) W. Ma, Y. Li, C. Y. H. Chao, C. Y. Tso, B. Huang, W. Li, S. Yao, *Cell Rep. Phys. Sci.* **2021**, *2*, 100384; b) E. Mitridis, T. M. Schutzius, A. Sicher, C. U. Hail, H. Eghlidi, D. Poulikakos, *ACS Nano* **2018**, *12*, 7009.
[49] J. Li, Y. Zhou, W. Wang, C. Xu, L. Ren, *Langmuir* **2020**, *36*, 1075.
[50] a) K. K. Varanasi, T. Deng, J. D. Smith, M. Hsu, N. Bhate, *Appl. Phys. Lett.* **2010**, *97*, 234102; b) W. Ma, Y. Li, S.-H. Yao, B.-L. Huang, *Acta Phys. Sin.* **2022**, *71*, 089201; c) Y. Peng, W. Zhao, F. Ni, W. Yu, X. Liu, *ACS Nano* **2021**, *15*, 19490.
[51] Y. Liu, L. Moevius, X. Xu, T. Qian, J. M. Yeomans, Z. Wang, *Nat. Phys.* **2014**, *10*, 515.
[52] a) J. B. Boreyko, C. P. Collier, *ACS Nano* **2013**, *7*, 1618; b) X. Chen, J. Wu, R. Ma, M. Hua, N. Koratkar, S. Yao, Z. Wang, *Adv. Funct. Mater.* **2011**, *21*, 4617; c) S. Zhang, J. Huang, Y. Tang, S. Li, M. Ge, Z. Chen, K. Zhang, Y. Lai, *Small* **2017**, *13*, 1600687.
[53] a) D. K. Sarkar, M. Farzaneh, *J. Adhes. Sci. Technol.* **2009**, *23*, 1215; b) Y. Zhang, E. Anim-Danso, S. Bekele, A. Dhinojwala, *ACS Appl. Mater. Interfaces* **2016**, *8*, 17583.
[54] Y. Zhao, C. Yan, T. Hou, H. Dou, H. Shen, *ACS Appl. Mater. Interfaces* **2022**, *14*, 26077.
[55] Y. Liu, R. Xu, N. Luo, Y. Liu, Y. Wu, B. Yu, S. Liu, F. Zhou, *Adv. Mater. Technol.* **2021**, *6*, 2100371.
[56] a) M. Elimelech, W. A. Phillip, *Science* **2011**, *333*, 712; b) M. A. Shannon, P. W. Bohn, M. Elimelech, J. G. Georgiadis, B. J. Mariñas, A. M. Mayes, *Nature* **2008**, *452*, 301; c) P. Wu, X. Wu, Y. Wang, H. Xu, G. Owens, *Chem. Eng. J.* **2022**, *435*, 134793; d) F. Peng, J. Xu, X. Bai, G. Feng, X. Zeng, M. R. Ibn Raihan, H. Bao, *Sol. Energy Mater. Sol. Cells* **2021**, *221*, 110910.
[57] G. Ni, G. Li, S V. Boriskina, H. Li, W. Yang, T. Zhang, G. Chen, *Nat. Energy* **2016**, *1*, 16126.
[58] N. Xu, J. Li, Y. Wang, C. Fang, X. Li, Y. Wang, L. Zhou, B. Zhu, Z. Wu, S. Zhu, J. Zhu, *Sci. Adv.* **2019**, *5*, eaaw7013.
[59] G. Li, W.-C. Law, K. C. Chan, *Green Chem.* **2018**, *20*, 3689.
[60] B. Zhang, P. W. Wong, J. Guo, Y. Zhou, Y. Wang, J. Sun, M. Jiang, Z. Wang, A. K. An, *Nat. Commun.* **2022**, *13*, 3315.
[61] L. Guterman, *Science* **2009**, *323*, 1558.
[62] J. Ge, L.-A. Shi, Y.-C. Wang, H.-Y. Zhao, H.-B. Yao, Y.-B. Zhu, Y. Zhang, H.-W. Zhu, H.-A. Wu, S.-H. Yu, *Nat. Nanotechnol.* **2017**, *12*, 434.
[63] a) C. Wu, X. Huang, X. Wu, R. Qian, P. Jiang, *Adv. Mater.* **2013**, *25*, 5658; b) C. Ruan, K. Ai, X. Li, L. Lu, *Angew. Chem.* **2014**, *126*, 5662; c) S. Singh, R. Jelinek, *Carbon* **2020**, *160*, 196; d) Y. Wang, L. Zhou, X. Luo, Y. Zhang, J. Sun, X. Ning, Y. Yuan, *J. Cleaner Prod.* **2019**, *230*, 995.
[64] J. Zhao, Z. Yin, M. Usman Shahid, H. Xing, X. Cheng, Y. Fu, S. Lu, *J. Hazard. Mater.* **2019**, *380*, 120625.
[65] X. Wu, Y. Lei, S. Li, J. Huang, L. Teng, Z. Chen, Y. Lai, *J. Hazard. Mater.* **2021**, *403*, 124090.
[66] M. Yu, P. Xu, J. Yang, L. Ji, C. Li, *Adv. Mater. Interfaces* **2020**, *7*, 1901671.
[67] H. Niu, J. Li, X. Wang, F. Luo, Z. Qiang, J. Ren, *ACS Appl. Mater. Interfaces* **2021**, *13*, 21175.
[68] X. Wang, L. Dai, N. Jiao, S. Tung, L. Liu, *Chem. Eng. J.* **2021**, *422*, 129394.
[69] S. Jiang, F. Liu, A. Lerch, L. Ionov, S. Agarwal, *Adv. Mater.* **2015**, *27*, 4865.
[70] B. Han, Y.-L. Zhang, L. Zhu, Y. Li, Z.-C. Ma, Y.-Q. Liu, X.-L. Zhang, X.-W. Cao, Q.-D. Chen, C.-W. Qiu, H.-B. Sun, *Adv. Mater.* **2019**, *31*, 1806386.

[71] F. Wang, J.-H. Jeon, S. Park, C.-D. Kee, S.-J. Kim, I.-K. Oh, *Soft Matter* **2016**, *12*, 246.
[72] W. Gao, L. Wang, X. Wang, H. Liu, *ACS Appl. Mater. Interfaces* **2016**, *8*, 14182.
[73] D.-D. Han, Y.-L. Zhang, Y. Liu, Y.-Q. Liu, H.-B. Jiang, B. Han, X.-Y. Fu, H. Ding, H.-L. Xu, H.-B. Sun, *Adv. Funct. Mater.* **2015**, *25*, 4548.
[74] a) B. Han, Y. L. Zhang, Q. D. Chen, H. B. Sun, *Adv. Funct. Mater.* **2018**, *28*, 1802235; b) Y. Yang, Y. Shen, *Adv. Opt. Mater.* **2021**, *9*, 2100035.
[75] D. Okawa, S. J. Pastine, A. Zettl, J. M. J. Fréchet, *J. Am. Chem. Soc.* **2009**, *131*, 5396.
[76] a) C. Maggi, F. Saglimbeni, M. Dipalo, F. De Angelis, R. Di Leonardo, *Nat. Commun.* **2015**, *6*, 7855; b) R.-L. Yang, Y.-J. Zhu, F.-F. Chen, D.-D. Qin, Z.-C. Xiong, *ACS Sustainable Chem. Eng.* **2019**, *7*, 13226.
[77] a) X. Song, X. Huang, J. Luo, B. Long, W. Zhang, L. Wang, J. Gao, H. Xue, *Nanoscale* **2021**, *13*, 12017; b) R.-L. Yang, Y.-J. Zhu, D.-D. Qin, Z.-C. Xiong, *ACS Appl. Mater. Interfaces* **2019**, *12*, 1339.
[78] W. Wang, Y.-Q. Liu, Y. Liu, B. Han, H. Wang, D.-D. Han, J.-N. Wang, Y.-L. Zhang, H.-B. Sun, *Adv. Funct. Mater.* **2017**, *27*, 1702946.
[79] a) P. Li, A. Wang, J. Fan, Q. Kang, P. Jiang, H. Bao, X. Huang, *Adv. Funct. Mater.* **2021**, *32*, 2109542; b) R. A. Kishore, A. Nozariasbmarz, B. Poudel, M. Sanghadasa, S. Priya, *Nat. Commun.* **2019**, *10*, 1765.
[80] C. Tan, Z. Dong, Y. Li, H. Zhao, X. Huang, Z. Zhou, J.-W. Jiang, Y.-Z. Long, P. Jiang, T.-Y. Zhang, B. Sun, *Nat. Commun.* **2020**, *11*, 3530.
[81] Z. Guo, C. Sun, J. Wang, Z. Cai, F. Ge, *ACS Appl. Mater. Interfaces* **2021**, *13*, 8851.
[82] K. Tang, K. Dong, J. Li, M. P. Gordon, F. G. Reichertz, H. Kim, Y. Rho, Q. Wang, C.-Y. Lin, C. P. Grigoropoulos, A. Javey, J. J. Urban, J. Yao, R. Levinson, J. Wu, *Science* **2021**, *374*, 1504.
[83] X. Yue, M. He, T. Zhang, D. Yang, F. Qiu, *ACS Appl. Mater. Interfaces* **2020**, *12*, 12285.
[84] a) J. He, R. Zhou, Y. Zhang, W. Gao, T. Chen, W. Mai, C. Pan, *Adv. Funct. Mater.* **2022**, *32*, 2107281; b) P. Xiao, W. Zhou, Y. Liang, S.-W. Kuo, Q. Yang, T. Chen, *Adv. Funct. Mater.* **2022**, *32*, 2201812.
[85] T. Q. Trung, N.-E. Lee, *Adv. Mater.* **2016**, *28*, 4338.
[86] H. Zhao, L. Hou, S. Bi, Y. Lu, *ACS Appl. Mater. Interfaces* **2017**, *9*, 33059.
[87] E. Pakdel, W. Xie, J. Wang, S. Kashi, J. Sharp, Q. Zhang, R. J. Varley, L. Sun, X. Wang, *Chem. Eng. J.* **2022**, *433*, 133688.
[88] J. Luo, S. Gao, H. Luo, L. Wang, X. Huang, Z. Guo, X. Lai, L. Lin, R. K. Y. Li, J. Gao, *Chem. Eng. J.* **2021**, *406*, 126898.
[89] K. G. Andersen, A. Rambaut, W. I. Lipkin, E. C. Holmes, R. F. Garry, *Nat. Med.* **2020**, *26*, 450.
[90] a) S. Ullah, A. Ullah, J. Lee, Y. Jeong, M. Hashmi, C. Zhu, K. I. Joo, H. J. Cha, I. S. Kim, *ACS Appl. Nano Mater.* **2020**, *3*, 7231; b) H. Shen, K. K. Leonas, *International Nonwovens Journal* **2005**, *os-14*, 1558925005os.
[91] a) L. Song, L. Sun, J. Zhao, X. Wang, J. Yin, S. Luan, W. Ming, *ACS Appl. Bio Mater.* **2019**, *2*, 2756; b) W. Deng, Y. Sun, X. Yao, K. Subramanian, C. Ling, H. Wang, S. S. Chopra, B. B. Xu, J. X. Wang, J. F. Chen, D. Wang, H. Amancio, S. Pramana, R. Ye, S. Wang, *Adv. Sci.* **2022**, *9*, 2102189; c) S. Kumar, M. Karmacharya, S. R. Joshi, O. Gulenko, J. Park, G.-H. Kim, Y.-K. Cho, *Nano Lett.* **2020**, *21*, 337.
[92] H. Zhong, Z. Zhu, J. Lin, C. F. Cheung, V. L. Lu, F. Yan, C.-Y. Chan, G. Li, *ACS Nano* **2020**, *14*, 6213.
[93] R. Soni, S. R. Joshi, M. Karmacharya, H. Min, S.-K. Kim, S. Kumar, G.-H. Kim, Y.-K. Cho, C. Y. Lee, *ACS Appl. Nano Mater.* **2021**, *4*, 8491.
[94] S. Li, P. Xiao, W. Zhou, Y. Liang, S.-W. Kuo, T. Chen, *Nano-Micro Lett.* **2022**, *14*, 32.

Shan Li is a Ph.D. student at the Ningbo Institute of Materials Technology and Engineering (NIMTE), Chinese Academy of Sciences, under the supervision of Professor Tao Chen. Her current research interests include superhydrophobic carbon-based hybrid functional films and their applications in flexible energy management and photothermal actuators.

Peng Xiao received his Ph.D. degree in 2017 from the University of Chinese Academy of Sciences. He is currently an associate professor at the Ningbo Institute of Materials Technology and Engineering NIMTE), Chinese Academy of Sciences. His current research interests focus on the design of carbon-based photothermal polymeric composites and their applications in multifunctional thermal management devices.

Tao Chen (Fellow of the Royal Society of Chemistry, FRSC) received his Ph.D. from Zhejiang University in 2006. After his postdoctoral training at the University of Warwick (UK), he joined Duke University (USA) as a research scientist. He then moved to Technische Universität Dresden (Germany) as an Alexander von Humboldt research fellow. Since 2012, he has been a professor at the Ningbo Institute of Materials Technology and Engineering (NIMTE), Chinese Academy of Sciences. He has published more than 200 papers in the fields of functional polymers. His research interests include photothermal composites with applications in actuators and thermal management etc.